© 2013. Published by The Company of Biologists Ltd | Development (2013) 140, 4554-4564 doi:10.1242/dev.098145

RESEARCH ARTICLE

Cxcl12/Cxcr4 signaling controls the migration and process orientation of A9-A10 dopaminergic neurons

Shanzheng Yang[1], Linda C. Edman[1], Juan Antonio Sánchez-Alcañiz[2], Nicolas Fritz[1], Sonia Bonilla[1,3], Jonathan Hecht[4,5], Per Uhlén[1], Samuel J. Pleasure[4], J. Carlos Villaescusa[1], Oscar Marín[2] and Ernest Arenas[1,*]

ABSTRACT

CXCL12/CXCR4 signaling has been reported to regulate three essential processes for the establishment of neural networks in different neuronal systems: neuronal migration, cell positioning and axon wiring. However, it is not known whether it regulates the development of A9-A10 tyrosine hydroxylase positive (TH^+) midbrain dopaminergic (mDA) neurons. We report here that *Cxcl12* is expressed in the meninges surrounding the ventral midbrain (VM), whereas CXCR4 is present in $NURR1^+$ mDA precursors and mDA neurons from E10.5 to E14.5. CXCR4 is activated in $NURR1^+$ cells as they migrate towards the meninges. Accordingly, VM meninges and CXCL12 promoted migration and neuritogenesis of TH^+ cells in VM explants in a CXCR4-dependent manner. Moreover, *in vivo* electroporation of *Cxcl12* at E12.5 in the basal plate resulted in lateral migration, whereas expression in the midline resulted in retention of TH^+ cells in the IZ close to the midline. Analysis of $Cxcr4^{-/-}$ mice revealed the presence of VM TH^+ cells with disoriented processes in the intermediate zone (IZ) at E11.5 and marginal zone (MZ) at E14. Consistently, pharmacological blockade of CXCR4 or genetic deletion of *Cxcr4* resulted in an accumulation of TH^+ cells in the lateral aspect of the IZ at E14, indicating that CXCR4 is required for the radial migration of mDA neurons *in vivo*. Altogether, our findings demonstrate that CXCL12/CXCR4 regulates the migration and orientation of processes in A9-A10 mDA neurons.

KEY WORDS: Midbrain, Dopamine, Migration, Neuritogenesis, Mouse

INTRODUCTION

Chemokines (chemotactic cytokines) constitute a family of small protein ligands that are classified into four major groups (referred to as C, CC, CXC and CX3C), based on the location and organization of their cysteine residues. The CXC members, also called α-chemokine subfamily, have a single amino acid residue between the first two conserved cysteine residues (Zlotnik and Yoshie, 2000). CXCL12 (stromal cell-derived factor 1/SDF1) is a member of the α-chemokine subfamily and, together with its cognate receptor, CXCR4, represent the best-known chemokine ligand/receptor pair.

Interestingly, besides their involvement in a battery of processes in the immune system, chemokines and their receptors are expressed by all major cell types in the central nervous system (CNS), and a growing body of evidence shows that chemokines and their receptors mediate cellular communication in the CNS (Mélik-Parsadaniantz and Rostène, 2008; Mithal et al., 2012; Zhu and Murakami, 2012). For example, projection neurons in the intermediate zone (IZ)/subventricular zone (SVZ) of the cortex express *Cxcl12* (Stumm and Höllt, 2007; Tiveron et al., 2006), and regulate the tangential migration of *Cxcr4*-expressing GABAergic interneurons (López-Bendito et al., 2008; Tiveron et al., 2006). In addition, *Cxcl12* is persistently expressed in the leptomeninges (Paredes et al., 2006; Stumm et al., 2007), where it also regulates the tangential migration of GABAergic interneurons (López-Bendito et al., 2008) and hem-derived Cajal-Retzius cells throughout the marginal zone (MZ) of the cortex (Borrell and Marín, 2006; Paredes et al., 2006). CXCL12/CXCR4 signaling is also responsible for the migration, assembly and positioning of cerebellar granule and Purkinje neurons (Ma et al., 1998), olfactory neurons (Miyasaka et al., 2007), as well as facial motoneurons (Sapède et al., 2005). Moreover, CXCL12/CXCR4 signaling is required for guiding the initial trajectory of ventral motoneurons (Lieberam et al., 2005) and for axon pathfinding of retinal ganglion cells and olfactory neurons (Li et al., 2005; Miyasaka et al., 2007). Similarly, the migration and final position of trigeminal and dorsal root ganglion cells, as well as their target innervation also require CXCL12/CXCR4 (Balabanian et al., 2005; Knaut et al., 2005; Odemis et al., 2005). Thus, CXCL12/CXCR4 signaling regulates the three key processes essential for the establishment of neural networks in different neuronal systems: neuronal migration, cell positioning and axon wiring.

Dopaminergic (DA) neurons, residing in the ventral midbrain (VM), are known to sequentially follow radial and tangential migration routes (Hanaway et al., 1971; Kawano et al., 1995), send long axonal processes and establish complex networks that regulate functions as diverse as control of voluntary movements, emotions and cognition (Ikemoto and Panksepp, 1999). The early development of mDA neurons has received much attention in recent years, particularly with regard to morphogenesis, progenitor specification, neurogenesis mDA differentiation and neuritogenesis (Andersson et al., 2013; Blakely et al., 2011; Deng et al., 2011; Inestrosa and Arenas, 2010; Prakash and Wurst, 2006; Di Salvio et al., 2010; Smits et al., 2006; Theofilopoulos et al., 2013; Van den Heuvel and Pasterkamp, 2008). However, very little is known about the molecular players that regulate the migration of mDA neurons. As adult mDA neurons express *Cxcr4* and this receptor modulates DA neurotransmission and the activity of the nigrostriatal pathway in response to CXCL12 (Guyon et al., 2008; Skrzydelski et al.,

[1]Laboratory of Molecular Neurobiology, Department of Medical Biochemistry and Biophysics, Karolinska Institutet, Scheeles väg 1, 17177 Stockholm, Sweden. [2]Instituto de Neurociencias, Consejo Superior de Investigaciones Científicas y Universidad Miguel Hernández, 03550 Sant Joan d'Alacant, Spain. [3]Universidad Europea de Madrid, Facultad de Ciencias Biomédicas, Departamento de Ciencias Biomédicas Básicas, Villaviciosa de Odón, 28670 Madrid, Spain. [4]Department of Neurology, University of California, San Francisco, CA 94143, USA. [5]Department of Pediatrics, University of California, San Francisco, CA 94143, USA.

*Author for correspondence (ernest.arenas@ki.se)

Received 30 April 2013; Accepted 30 August 2013

Development (2013) doi:10.1242/dev.098145

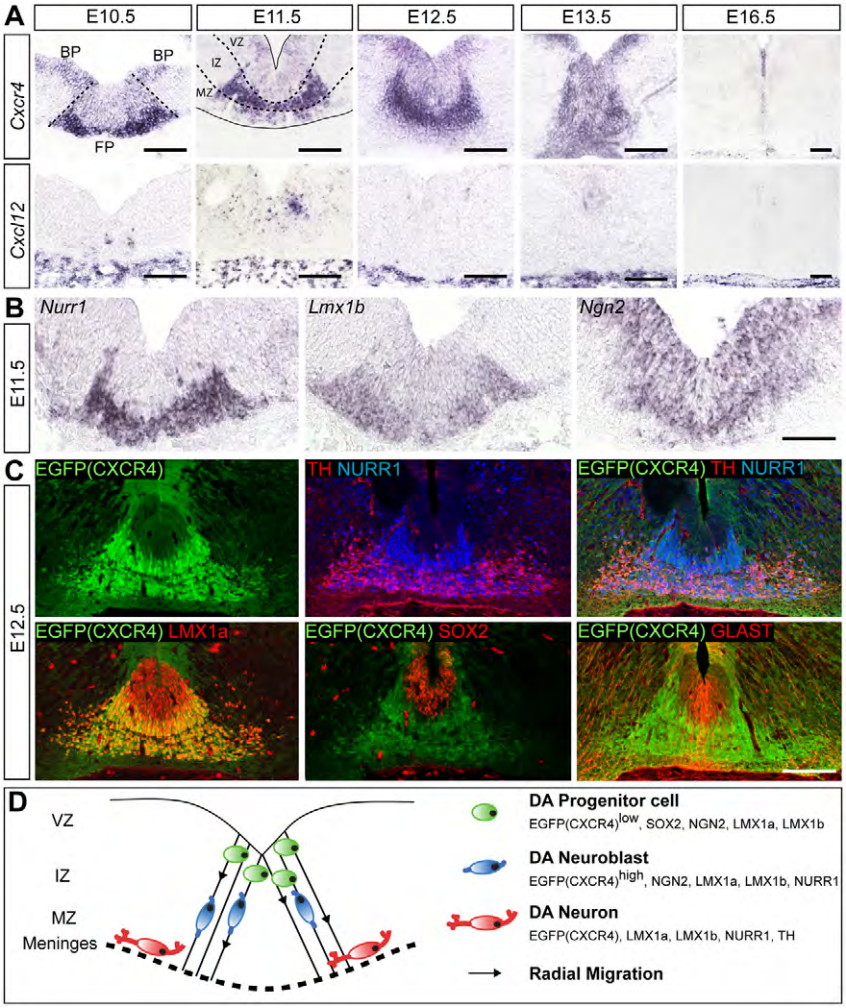

Fig. 1. Cxcl12 and Cxcr4 are expressed in the developing midbrain. (A) *In situ* hybridization at E10.5 to E16.5 revealed that Cxcr4 was expressed in the ventral midline region of the midbrain during development, and that Cxcl12 was expressed in the meninges surrounding the midbrain during the same developmental stages. (B) *In situ* hybridization at E11.5 also revealed that *Nurr1*, *Lmx1b* and *Ngn2* shared coinciding expression patterns to that of *Cxcr4*. (C) At E12.5, double immunohistochemistry on *Cxcr4-Egfp* BAC transgenic mice brains revealed that EGFP was co-expressed with NURR1, TH, LMX1A and SOX2. $EGFP^+$ cells were also shown to migrate along $GLAST^+$ radial glia cells. (D) The distribution of EGFP in the three main different cell types layers in the mDA lineage. Scale bars: 200 µm. FP, floorplate; BP, basal plate; VZ, ventricular zone; IZ, intermediate zone; MZ, marginal zone.

2007), we sought to determine whether CXCL12 also works to regulate the migration of mDA neurons during development. We hereby demonstrate that CXCL12/CXCR4 signaling regulates both the initial orientation and the migration of A9-A10 mDA neurons.

RESULTS

Cxcr4 and *Cxcl12* are expressed in the developing ventral midbrain

To study the spatial and temporal expression of *Cxcr4* and its ligand, *Cxcl12*, during the course of mDA neuron development, we performed *in situ* hybridization using mouse VM tissue at different embryonic (E) stages (E10.5, E11.5, E12.5, E13.5 and E16.5). We found that *Cxcr4* was strongly expressed in the floor plate region of the midbrain already at E10.5, at the onset of mDA neurogenesis. At E11.5, the expression was strongest in the intermediate zone (IZ), compared with the ventricular zone (VZ) and the marginal zone (MZ). This expression pattern was conserved at E12.5, become more homogenous at E13.5 and nearly disappeared at E16.5 (Fig. 1A, upper row). By contrast, we found that *Cxcl12* is expressed in the meninges surrounding the VM during all these developmental stages, from E10.5 to E16.5 (Fig. 1A, lower row). To characterize the cell compartment that expressed *Cxcr4*, we performed additional *in situ* hybridization for three genes encoding well-known mDA transcription factors: *Ngn2*, which is expressed in mDA progenitors and neuroblasts (Kele et al., 2006); *Lmx1b*, which is expressed at low levels in mDA progenitors and at high levels in mDA neuroblasts and neurons (Smidt et al., 2000); and *Nurr1*, which is a nuclear receptor expressed by postmitotic mDA neuroblasts and neurons (Castillo et al., 1998; Saucedo-Cardenas et al., 1998; Zetterström et al., 1997; Castillo et al., 1998; Saucedo-Cardenas et al., 1998; Zetterström et al., 1997). *Cxcr4* expression was very similar to that of *Lmx1b*, and the area of high *Cxcr4* expression level coincided with that of *Nurr1* expression at E11.5 (Fig. 1B). These findings suggested that mDA neuroblasts in the IZ and mDA neurons in the MZ both express *Cxcr4*. To ascribe precisely the expression of *Cxcr4* to specific cell types within the mDA lineage, we took advantage of a transgenic mouse strain in which *EGFP* is expressed under the *Cxcr4* promoter (Gong et al., 2003). Double immunohistochemistry experiments using different mDA markers such as NURR1, tyrosine hydroxylase (TH), the rate-limiting enzyme for DA synthesis (Albéri et al., 2004; Kawano et al., 1995), and LMX1A, a transcription factor that is expressed in all cells in the mDA lineage (Andersson et al., 2006), revealed that EGFP is mainly found in postmitotic cells (Fig. 1C). At E12.5, for example, EGFP was found in mDA neuroblasts ($NURR1^+/TH^-$), as well as in mDA neurons ($NURR1^+/TH^+$). High levels of EGFP were also detected in $LMX1A^+$ cells in the IZ and MZ of the floor plate, but not in the VZ of the floor plate (Fig. 1C). Interestingly, SOX2, a HMG-box transcription factor (Kele et al., 2006), and GLAST (glutamate astrocyte transporter), a radial glia marker (Bonilla et al., 2008), were mainly found in basal plate or midline EGFP cell bodies and processes (Fig. 1C,D). These observations suggest that as mDA

Development (2013) doi:10.1242/dev.098145

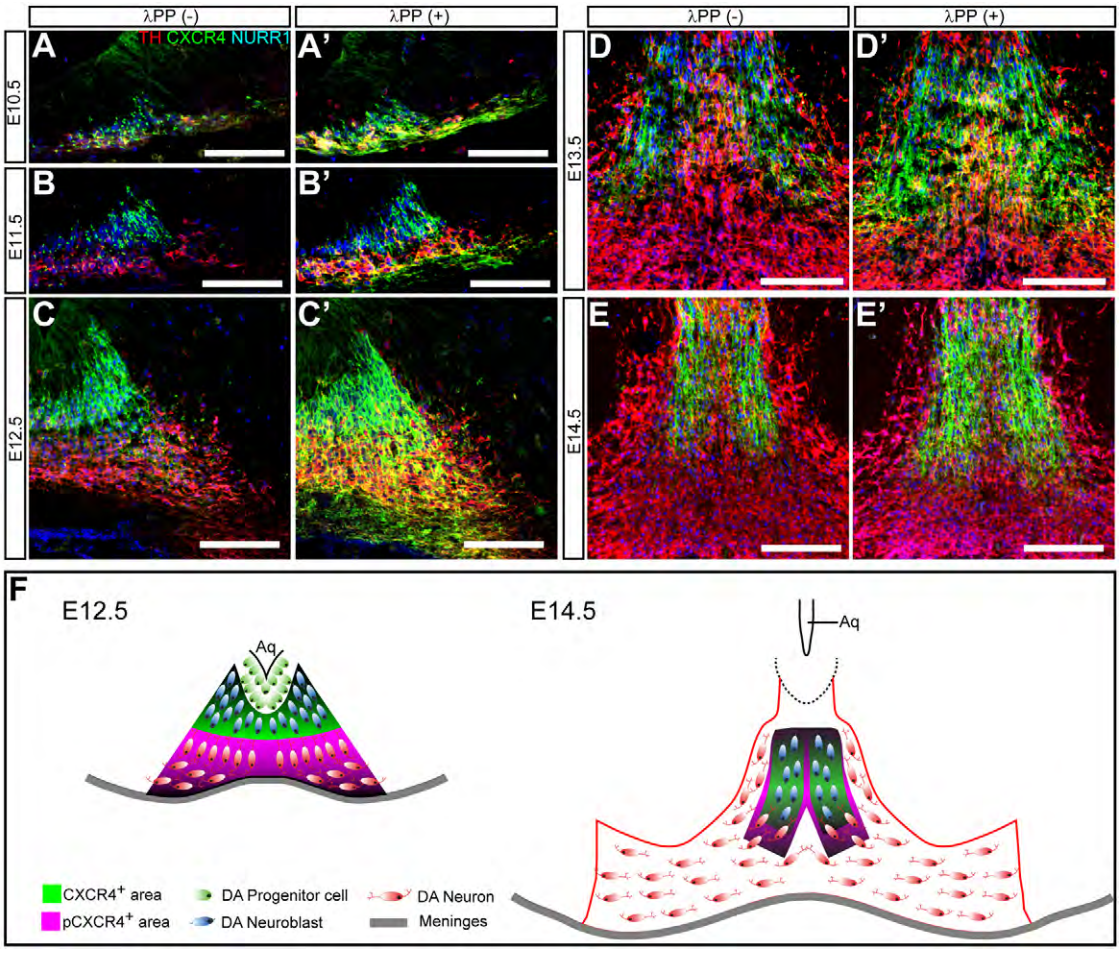

Fig. 2. CXCR4 is phosphorylated in midbrain DA neuroblasts and neurons. CXCR4 protein was detected by immunohistofluorescence staining with a de-phospho CXCR4 antibody (UMB-2) on mouse midbrain sections at rostrocaudal intermediate levels from E10.5, E11.5, E12.5, E13.5 and E14.5 (A-E, respectively). After treatment with λ protein phosphatase (λPP), phosphorylated CXCR4 protein was unraveled and detected as an extended area with the de-phospho CXCR4 antibody in consecutive sections (A′-E′, respectively). (F) The developmental changes in the patterns of CXCR4 immunoreactive staining before and after λ protein phosphatase treatment. Scale bars: 100 μm. Aq, aqueduct.

progenitors in the floor plate undergo neurogenesis and give rise to mDA neuroblasts, they upregulate the expression of *Cxcr4* and initiate their radial migration. Thus, the upregulation of *Cxcr4* could provide mDA precursors with competence to respond to directional cues produced by the meninges, such as CXCL12.

CXCR4 is expressed and phosphorylated in migrating NURR1$^+$ cells

Given that the turnover of EGFP and CXCR4 may be different, we first examined the presence of CXCR4 protein by immunohistochemistry using a highly specific rabbit monoclonal antibody (Fischer et al., 2008). Consistent with the mRNA expression pattern (Fig. 1A, upper row), CXCR4 protein was mainly detected in the IZ of midbrain floor plate during the entire period of mDA neurogenesis: at high levels from E10.5 to E12.5 (Fig. 2A-C); at lower levels and in fewer cells from E13.5 to E14.5 (Fig. 2D-E); and almost absent at E16.5 (data not shown).

CXCR4, like other G protein-coupled receptors (GPCR), is activated when binding to its ligand, CXCL12, which leads to the phosphorylation of its C-terminal domain (Gerlach et al., 2001; Hatse et al., 2002; Rubin et al., 2003; Schols et al., 1997). Interestingly, the antibody that we used recognizes only the non-phosphorylated form of CXCR4 (Sánchez-Alcañiz et al., 2011), i.e. the receptor that has not yet been activated. In order to be able to identify in which cells the receptor had been activated, we performed immunohistochemistry in phosphatase-treated (λPP+) consecutive sections (Fig. 2A′-E′). To our surprise, we found not only higher levels of CXCR4 in NURR1$^+$ cells of the IZ, but also many TH$^+$ cell bodies and fibers in the MZ of phosphatase-treated sections, particularly at E12.5. Consistently, immunostaining with antibodies against phosphorylated S324/325 and S338/339 of CXCR4 also showed the localization of phosphorylated CXCR4 in TH$^+$ neurons (supplementary material Fig. S1). These results revealed that CXCR4 begins its activation in NURR1$^+$/TH$^-$ neuroblasts of the IZ and is fully activated in most NURR1$^+$/TH$^+$ mDA neurons of the MZ by E12.5, as they move closer to the meninges.

Ventral midbrain meninges promote the migration and neuritogenesis of TH$^+$ cells *in vitro* via CXCR4

To study the function of the meninges, we first performed meningeal ablation experiments in organotypic cultures from E12.5 midbrain and examined the position of TH$^+$ cells and their processes. Notably, we found an increase in the number of TH$^+$ cells migrating away

Development (2013) doi:10.1242/dev.098145

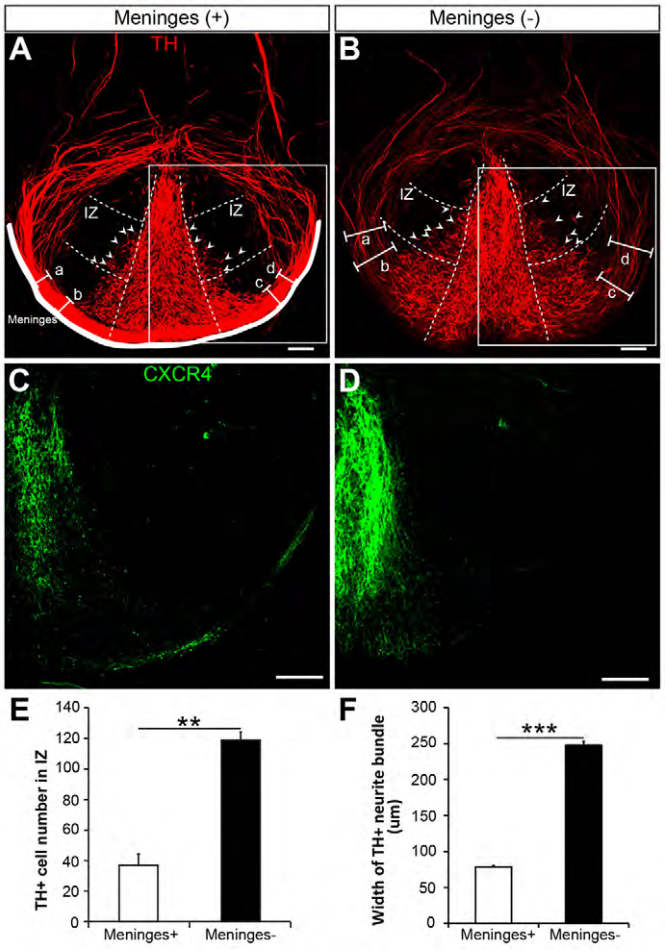

Fig. 3. Ablation of meninges causes defects in radial migration of TH$^+$ cells and the fasciculation of TH$^+$ processes in E12.5 VM organotypic cultures. (A-D) Vibrotome sections from E12.5 mouse midbrain were cultured with (A,C) or without (B,D) meninges attached for 2 days *in vitro*. (A,B) TH$^+$ cells migrated laterally in the IZ of cultures (meninges– versus meninges+). Arrowheads indicate the most lateral TH$^+$ cell bodies in the IZ compartment. (C,D) Non-phosphorylated CXCR4 was detected at higher levels and over a broader domain in cultures without meninges. (E) Quantification of the number TH$^+$ cells revealed an increase in IZ. (F) The width of the TH$^+$ process bundle (average in positions a-d in A,B) was increased (meninges– versus meninges+). Scale bars: 100 μm. $^{**}P<0.01$, $^{***}P<0.001$, *t*-test ($n=3$).

from the midline, which was detectable even in the IZ (Fig. 3A,B,E), and an increase non-phosphorylated CXCR4 (Fig. 3C,D). Additionally, we also found that the width of the bundles formed by TH$^+$ process near the meninges increased in VM slices without meninges compared with the ones with meninges (Fig. 3A,B,F). These results suggested that the meninges regulate both the migration of TH$^+$ cell bodies and the fasciculation of their axons in organotypic cultures.

We next examined whether the meninges are capable of promoting the migration of TH$^+$ cells in a CXCR4-dependent manner and performed co-cultures of E11.5 or E12.5 meninges and VM explants treated with the CXCR4 antagonist, AMD3100 or vehicle. We found that the meninges induced the migration of TH$^+$ cell bodies (TH$^+$/TOPRO3$^+$ cells) from E11.5 or E12.5 explants, compared with their corresponding contralateral side (Fig. 4A,C; arrowheads in Fig. 4a,a′,c,c′). The effect of meninges declined with the distance to the VM explant (supplementary material Fig. S2). Moreover, migration was blocked by administration of AMD3100 at both stages (Fig. 4B,D,E; arrowheads in Fig. 4b,b′,d,d′). These results indicated that CXCR4 regulates the migration of TH$^+$ cells *in vitro*.

As E11.5 mDA neurons extend their neurites first towards the meninges (Van den Heuvel and Pasterkamp, 2008), we next investigated whether neuritogenesis is also influenced by the meninges in a CXCR4-dependent manner. To test the effect of meningeal CXCL12 on this process, we cultured E11.5 or E12.5 midbrain organotypic slices with meningeal explants placed ventral and lateral to the VM midline (Fig. 4F-I). After 48 hours, meninges were found to exert a neuritogenic effect on the TH$^+$ cells (Fig. 4F,H), which was blocked by AMD3100 (Fig. 4G,I,J). Moreover, we found that *Cxcl12*-expressing COS7 cells promoted the growth of TH$^+$ neurites from VM explants in a similar manner to meningeal CXCL12 (Fig. 4K,L). These effects were also effectively blocked by the CXCR4 antagonist AMD3100 (Fig. 4M,N). Altogether, these results indicated that CXCL12/CXCR4 mediate the neuritogenic and migratory effects of the meninges on TH$^+$ mDA neurons *in vitro*.

Ectopic expression of *Cxcl12* redirects the migration of mDA neurons *in vivo*

Based on the pro-migratory effects of CXCL12 *in vitro* and the requirement of CXCR4 for this process, we hypothesized that ectopic expression of CXCL12 would attract postmitotic mDA neurons *in vivo*. We thus decided to perform *in utero* electroporations at E12.5, with plasmids encoding *Gfp* or *Cxcl12*, and examined the position of TH$^+$ cells at E14.5 (Fig. 5A). We first performed unilateral electroporations in the basal plate, to test directly whether CXCL12 was sufficient to redirect their migration. The number of TH$^+$ cells residing more than 500 μm away from the midline was counted. Although the number of lateral TH$^+$ cells in the *Gfp*-electroporated ipsi- and contralateral sides was similar, lateral TH$^+$ cells were more abundant in the side electroporated with *Cxcl12* (Fig. 5B-D). Moreover, the position of TH$^+$ cells ipsilateral to *Cxcl12* was more ventral, compared with either the contralateral side or control embryos electroporated with *Gfp* (Fig. 5B,C). These results indicate that CXCL12 indeed promotes the migration of TH$^+$ cells in the VM *in vivo*.

Next, we performed electroporation of *Gfp* or *Cxcl12* in the midbrain floor plate, to examine whether the expression of *Cxcl12* in the midline would enhance or prevent the proper migration of mDA neurons. Notably, *Cxcl12* overexpression resulted in the retention of TH$^+$ mDA neurons in the ipsilateral IZ (open arrows in Fig. 5F) compared with *Gfp* (Fig. 5E-G). Simultaneously, less TH$^+$ neurons were found in the MZ ipsilateral to *Cxcl12* overexpression (Fig. 5E,F,H). These results thus show that CXCL12 works as an attractant that promotes the migration of mDA neurons towards CXCL12 sources *in vivo*. Indeed, we found that distant (lateral) sources of CXCL12 attracted mDA neurons, whereas local (medial) sources retained them.

Inhibition of CXCR4 impairs the migration of mDA neurons *in vivo*

Based on the previous experiments, we hypothesized that CXCR4 may be required for the migration of mDA neurons *in vivo*. To address this hypothesis, we blocked CXCR4 function in the developing midbrain by injecting AMD3100 into the mesencephalic ventricle *in utero* at E11.5 and analyzed the distribution of mDA neurons 2 days after injection (Fig. 6). In control embryos, TH$^+$ mDA neurons

Development (2013) doi:10.1242/dev.098145

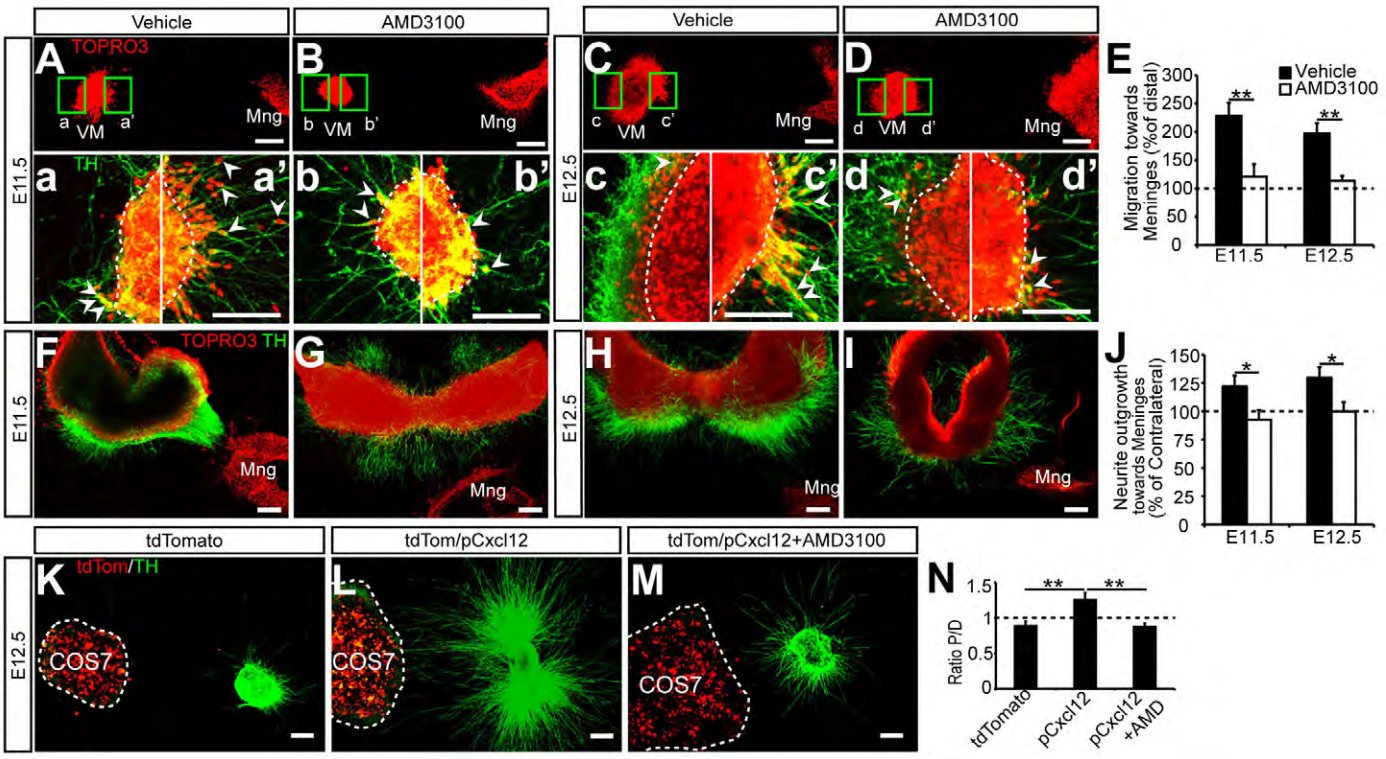

Fig. 4. Meninges promote the migration and neuritogenesis of dopaminergic neurons. The migration of TH$^+$ cells out of E11.5 and E12.5 VM tissue fragment (VM) confronted with a clump of meninges treated with or without the CXCR4 antagonist AMD3100 (B,b,b′ and A,a,a′, respectively) was examined. Boxed areas in A-D are magnified in a-d′, respectively. Arrowheads in a-d′ indicate the TH$^+$ cell bodies. (E) The ratio of the distance of TH$^+$ cells migrating away from the proximal to distal side to meninges was quantified. For E11.5, *n*=26 and 20 (vehicle and AMD3100, respectively). For E12.5, *n*=19 (vehicle or AMD3100). (F-I) Neurite outgrowth of TH$^+$ neurons from E11.5 (F,G) and E12.5 (H,I) VM sections (250 µm) confronted with meninges treated with (G,I) or without (F,H) AMD3100. (J) The ratio of the length of TH$^+$ neurite outgrowth in ipsilateral to contralateral side of VM sections to meninges was quantified. For E11.5, *n*=8 and 9 (vehicle and AMD3100, respectively). For E12.5, *n*=11 and 12 (vehicle and AMD3100, respectively). **P*<0.05, ***P*<0.01, *t*-test. (K-M) TH$^+$ neurite outgrowth from VM fragments confronted with COS cell aggregates (red) expressing tdTomato (K; *n*=27), tdTomato+Cxcl12 (L; *n*=22) or tdTomato+Cxcl12+AMD3100 (M; *n*=21). (N) Quantification of the neurite outgrowth ratio (proximal versus distal side of VM fragments). ***P*<0.01, one-way analysis of variance with Bonferroni post-hoc test. Scale bars: 200 µm.

adopted the classical ‘inverted fountain’ distribution in coronal sections of midbrain at E13.5 (Fig. 6A). To examine the distribution of mDA neurons, we divided each side of the VM into five domains (supplementary material Fig. S3): ventricular zone (VZ), midline, upper and lower intermediate zones (uIZ and lIZ, respectively), and marginal zone (MZ). Although most of the mDA neurons, identified by TH and PITX3 immunohistochemistry, were found the in midline and MZ compartments, very few were found in the IZ (Fig. 6A,B, intermediate levels). Immunohistochemistry against CXCR4, without or with λPP treatment (Fig. 6C,C′), revealed an expression pattern similar to that shown in Fig. 2G,G′, indicating that vehicle injection does not affect CXCR4, its phosphorylation or cell migration. By contrast, in AMD3100-injected embryos, large numbers of TH$^+$ (Fig. 6B) and PITX3$^+$ (Fig. 6D) cells were found in uIZ and lIZ, which suggested that CXCR4 receptor blockade impairs the correct migration of mDA neurons. Most notably, CXCR4 immunoreactivity (without λPP treatment, Fig. 6D) revealed a much broader staining area in AMD3100-injected embryos than in controls. By contrast, no obvious differences were found in CXCR4 staining after λPP treatment (Fig. 6D′), which reflected the fact that CXCR4 was effectively blocked by AMD3100.

We next quantified the number of TH$^+$ cells in midbrain sections through the entire midbrain and their distribution at three rostrocaudal levels, i.e. rostral, intermediate and caudal. Although the injection of AMD3100 did not affect the total number of TH$^+$ cells (Fig. 6E), it modified their distribution at different levels of the midbrain. Whereas AMD31000 increased the number of TH$^+$ cells in the uIZ and lIZ, from rostral to caudal levels, it decreased TH$^+$ in the MZ, at intermediate levels (Fig. 6F-H). These results suggested that CXCR4 blockade allows TH$^+$ cells to move prematurely laterally towards the intermediate zone, thereby decreasing the number of cells that reach the marginal zone.

Deletion of *Cxcr4* impairs the migration and process orientation of mDA neurons *in vivo*

To verify the previous findings, we next analyzed the distribution and number of TH$^+$ mDA neurons in *Cxcr4* mutant embryos at E11.5 and E14. At E11.5, nearly all TH$^+$ cells were located in the MZ of control embryos, whereas several cells were present in the IZ of *Cxcr4*$^{-/-}$ mice (Fig. 7A-D; open arrows in 7B). Although the total number of TH$^+$ cells in the VM of *Cxcr4*$^{-/-}$ embryos did not differ from controls (Fig. 7E), the proportion of cells retained in the IZ of *Cxcr4*$^{-/-}$ embryos was more than 10-fold higher than in controls (Fig. 7C,D,F). Consistent with our organotypic culture experiments, *in vivo* experiments showed that the number of mDA neurons in the IZ exhibiting elaborated and misguided processes (non-radially oriented, open arrowheads in Fig. 7D) was prominently increased (around 4-fold) in mutant embryos compared with control embryos

Development (2013) doi:10.1242/dev.098145

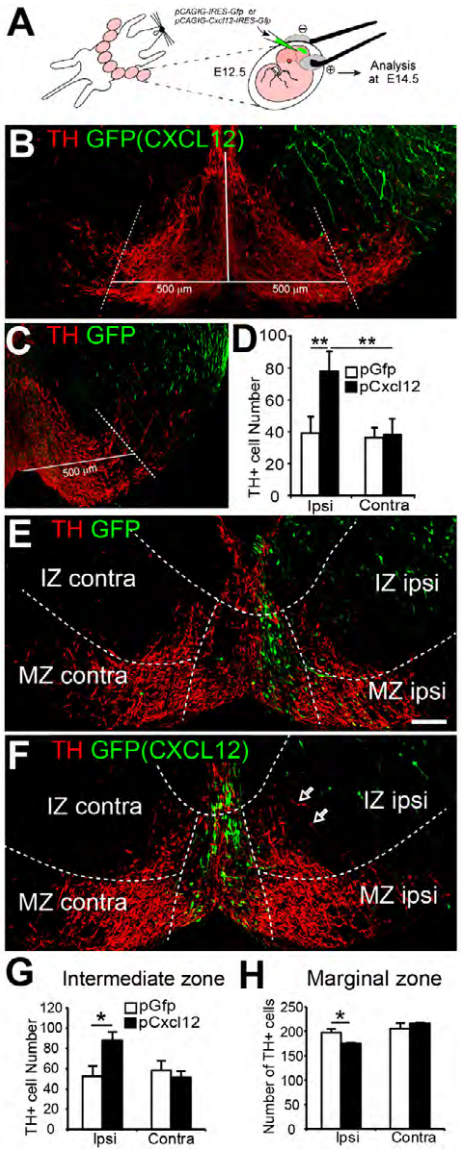

Fig. 5. Cxcl12 directs the migration of TH⁺ mDA neurons *in vivo*. (A) *pCAGIG-IRES-Cxcl12* or *pCAGIG-IRES-Gfp* was injected into the mesencephalic ventricle of E12.5 wild-type embryos *in utero*, and embryos were collected at E14.5. (B,C) Overexpression of *Cxcl12* (*n*=6) in the basal plate promoted the migration of TH⁺ mDA neurons away from the midline, when compared with control embryos (*n*=5). Cells residing 500 µm away from the midline, indicated by the dotted lines (B,C), were quantified (D). (E,F) Overexpression of *Cxcl12* in the midline caused the retention of TH⁺ cells in IZ (*n*=3). (G,H) Quantification of TH⁺ cell distribution in intermediate zone (IZ; G) and marginal zone (MZ; H). Each value represents the mean±s.e.m. **P*<0.05, ***P*<0.001, *t*-test. Scale bar in E: 100 µm in E,F.

(Fig. 7G). These results indicate that *Cxcr4* is required *in vivo* for the migration of mDA neurons.

To further confirm the involvement of CXCL12/CXCR4 in the migration of mDA neurons, we examined *Cxcr4* mutant embryos at E14. Analysis of the distribution of TH⁺ neurons in the VM compartments described in supplementary material Fig. S4 and Fig. 5 revealed that more TH⁺ cells were present in the upper and lower IZ of *Cxcr4* mutant brains than controls, at all three rostrocaudal levels (arrowheads in Fig. 8A). Of note, the expression of NURR1 or PITX3 (Fig. 8B) and the total number of TH⁺ cells (Fig. 8C) did not change, which indicated that the deletion of *Cxcr4* impairs migration, but not the differentiation of mDA neurons. In addition, a more-detailed analysis of the position of TH⁺ cells revealed a marked increase in the uIZ, where the number of TH⁺ cells increased ~7-fold (from 12 in $Cxcr4^{+/-}$ to 83 in $Cxcr4^{-/-}$, Fig. 8D-F). This increase was accompanied by a marked decrease in the number of TH⁺ cells in the MZ at intermediate level (Fig. 8E) and an abnormal positioning of TH⁺ cells in the most ventral aspect of the MZ at rostral and intermediate levels (asterisk in Fig. 8A). These results showed that, in the absence of CXCR4, some TH⁺ neurons move laterally, within the IZ, and do not reach the MZ. Additionally, we also observed that the neurites of TH⁺ cells in the lateral part of MZ were oriented more perpendicularly to the meninges in control $Cxcr4^{+/-}$ mice than in those in $Cxcr4^{-/-}$ embryos (supplementary material Fig. S4), a result that is consistent with the disorientation of TH⁺ processes at E11.5. Taken together, our results demonstrate that CXCR4 is required for the proper orientation of TH⁺ processes and for the radial migration of TH⁺ cells from the IZ to the MZ. Finally, as CXCR4 was detected at very low levels in radial glia of the midbrain floor-plate, we examined whether the defect in radial migration could be indirectly influenced by the radial glia. However, we found no alteration in the distribution or processes of radial glia in the midbrain floor plate, as assessed by NESTIN immunostaining in either $Cxcr4^{-/-}$ mice or after pharmacological inhibition of CXCR4 (supplementary material Fig. S5), suggesting that defect in radial migration of TH⁺ cells in $Cxcr4^{-/-}$ embryos is cell autonomous. Thus, combined, our data shows that the activation of CXCR4 in TH⁺ cells is both required and sufficient for the migration of mDA neurons *in vivo*.

DISCUSSION

Our results indicate that VM meninges regulate the radial migration and neuritogenesis in mDA neurons in a CXCR4-dependent manner. We show that *Cxcl12* is expressed in the meninges and its receptor, CXCR4, is present and it is activated (phosphorylated) in mDA neurons as they migrate ventrally through the intermediate zone of the VM, from E11.5 to E14.5. Moreover, we found that CXCL12 is sufficient to promote the migration and neuritogenesis of mDA neurons and that CXCR4 is required for these processes both *in vitro* and *in vivo*. Indeed, loss of CXCR4 function *in vivo*, in AMD3100-treated or in $Cxcr4^{-/-}$ embryos, perturbed the neuritogenesis and radial migration of mDA neurons towards the MZ and resulted in their misplacement in the IZ of the VM.

CXCL12 is widely expressed in developing brain (Lazarini et al., 2000; Liapi et al., 2008; Stumm et al., 2007; Tham et al., 2001), in particular in the meninges overlaying the cortex (Borrell and Marín, 2006; Stumm et al., 2007; Tissir et al., 2004), cerebellum (Reiss et al., 2002; Zhu et al., 2002), hippocampus (Lu et al., 2002) and spinal cord (Tysseling et al., 2011). In the present study, we found that *Cxcl12* is also expressed in the meninges covering the developing mesencephalon, which suggested that CXCL12/CXCR4 signaling could exert similar functions in this structure. Although CXCR4 was detected at very low level in GLAST⁺ radial glia and SOX2⁺ cells in the VM floorplate, strong levels of CXCR4 were detected in postmitotic cells of the IZ and MZ. Notably, CXCR4 was present in mDA neuroblasts and mDA neurons, as revealed by its colocalization with NURR1 and TH in the VM of wild-type mice and in *Cxcr4* BAC transgenic mice. In these experiments, immunohistochemistry was performed with the UMB-2 CXCR4 antibody (Fischer et al., 2008), which does not recognize the phosphorylated and active receptor (Sánchez-Alcañiz et al., 2011). However, comparison of sections with or without protein phosphatase treatment, as well as the use of phospho-specific

Development (2013) doi:10.1242/dev.098145

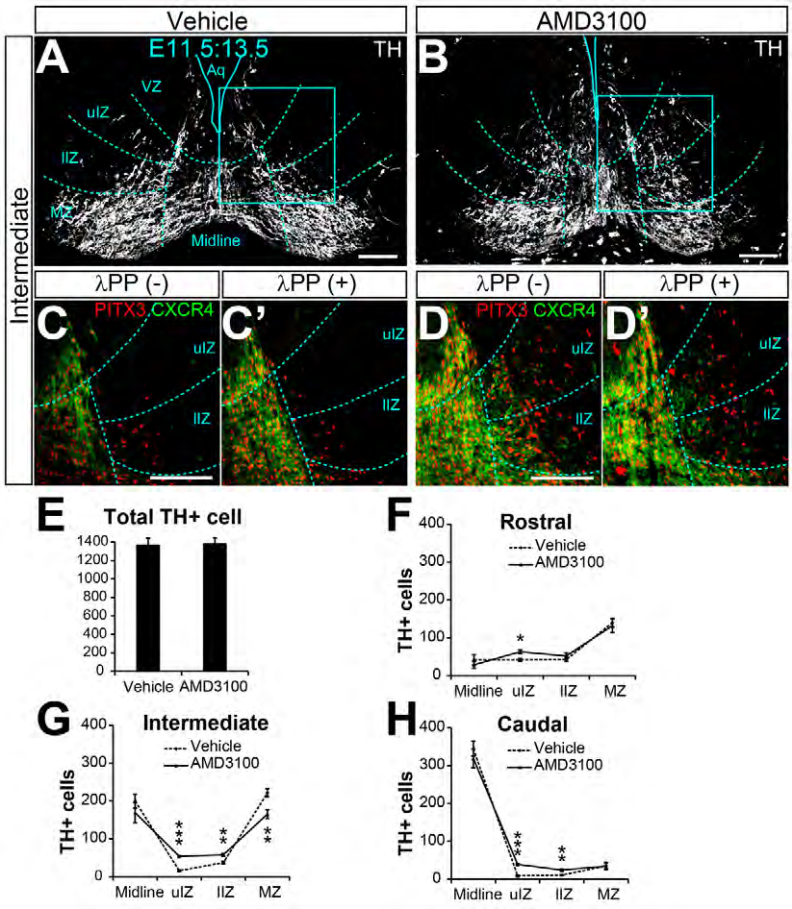

Fig. 6. Pharmacological inhibition of CXCR4 impairs the migration of mDA neurons *in vivo*. (A-D) The CXCR4 antagonist AMD3100 or vehicle (*n*=5 for each group) solution was injected into the mesencephalic ventricle of E11.5 embryos *in utero* and embryos were collected at E13.5. (A,B) Distribution of TH$^+$ cells in midbrain intermediate level of vehicle- or AMD3100-treated embryos, respectively. The VM was divided into eight compartments: ventricular (VZ), upper intermediate zone (uIZ), lower intermediate zone (lIZ), marginal zone (MZ) and midline region (A). More TH$^+$ cells were found in the IZ and fewer in the MZ of AMD3100-treated embryos (B). (C,C′) Consecutive sections were treated with (C′) or without λPP (C), and immunostained to show PITX3 (red) and increased CXCR4 (green) after λPP treatment. (D,D′) Consecutive sections of AMD3100-treated embryos were treated with (D′) or without λPP (D), and immunostained to show lateral displacement of PITX3$^+$ cells (red) and similar levels of CXCR4 (green) in areas corresponding to the box in B. (E) Quantification of the total TH$^+$ cell number in the midbrain shows no change after AMD3100 treatment. (F-H) Quantification of distribution of TH$^+$ cells in each compartment at rostral (F), intermediate (G) and caudal (H) levels. **P*<0.05, ***P*<0.01, ****P*<0.001, *t*-test. Scale bars: 100 μm.

antibodies (S324/325 and S338/339), allowed us to distinguish naïve (dephosphorylated) from active (phosphorylated) CXCR4. These experiments revealed that the active form of the receptor is present in both mDA neuroblasts, but mainly in the cell bodies and processes of TH$^+$ DA neurons. Notably, the UMB-2 antibody recognizes non-phosphorylated S346/347, a site whose phosphorylation is required for subsequent multi-site phosphorylation (S324 and S338/339) and is the main site for the functional regulation of CXCR4 (Mueller et al., 2013). It is also known that phosphorylation of Ser346-348 and Ser351 or Ser352 by CXCL12 treatment recruits arrestin 2 and/or arrestin 3, and activates Erk1/2 (Busillo et al., 2010) and p38 MAPK (Sun et al., 2002). The activation of the p38 MAPK pathway by arrestin 3 has been reported to mediate CXCL12-induced chemotaxis (Sun et al., 2002), a result that it is consistent with the idea that the phosphorylation of CXCR4 in mDA neurons may also regulate their migration.

In the developing CNS, CXCL12/CXCR4 signaling has been shown to regulate the migration and positioning of several types of neurons, including cerebellar granule cells, cortical interneurons and hindbrain pontine neurons (Zhu and Murakami, 2012). However, cell migration is regulated in different ways in these locations. Although CXCL12 secreted by meninges serves as an anchoring factor to retain proliferating cerebellar precursors in the external granule layer (Reiss et al., 2002; Zhu et al., 2002) and in the dentate gyrus of the hippocampus (Li et al., 2009), meningeal CXCL12 stimulates the migration of hem-derived Cajal-Retzius (CR) cells in the cerebral cortex (Borrell and Marín, 2006). What, then, is the role of CXCL12 in migration of mDA *in vivo*? In the present study, we observed that meningeal CXCL12 induces migration and neuritogenesis in mDA neurons in VM explant cultures and that pharmacological blockade of CXCR4 or genetic deletion of *Cxcr4* results in the retention of TH$^+$ mDA neurons in the upper intermediate zone of the VM at E14-14.5. Migration defects were already detected at E11.5 in *Cxcr4*$^{-/-}$ embryos and were very clear at E14, not only at the intermediate level of the marginal zone, where less cells were detected, but also in the rostral marginal zone, where TH$^+$ cells occupied an abnormally ventral position. These results, together with the absence of morphological abnormalities in radial glia and the presence of CXCR4 in mDA neuroblasts and neurons, suggests that the defect in migration of TH$^+$ cells is cell autonomous. Notably, ectopic expression of *Cxcl12 in vivo* regulated migration in different ways, depending on the position of the ectopic source of ligand. Although lateral expression of *Cxcl12* directed mDA neurons to migrate laterally, medial expression led to the retention of mDA neurons in the intermediate zone and prevented their proper migration to the marginal zone, a phenotype that actually resembled loss-of-function experiments. Based on these findings, we suggest that CXCL12/CXCR4 signaling may work as an attractant for midbrain mDA neurons and, because of the normal expression of CXCL12 in the meninges, that this system promotes the radial migration of postmitotic mDA cells towards the marginal zone.

Besides controlling the migration of neurons and their precursors, CXCL12 has also been reported to regulate axon pathfinding (Xiang et al., 2002; Li et al., 2005; Lerner et al., 2010) and axon elongation (Arakawa et al., 2003). Moreover, mDA neurons start extending neurites dorsally, at E11.5 (Blakely et al., 2011; Kolk et al., 2009), but they soon turn ventrally, towards the meninges, and form the

Development (2013) doi:10.1242/dev.098145

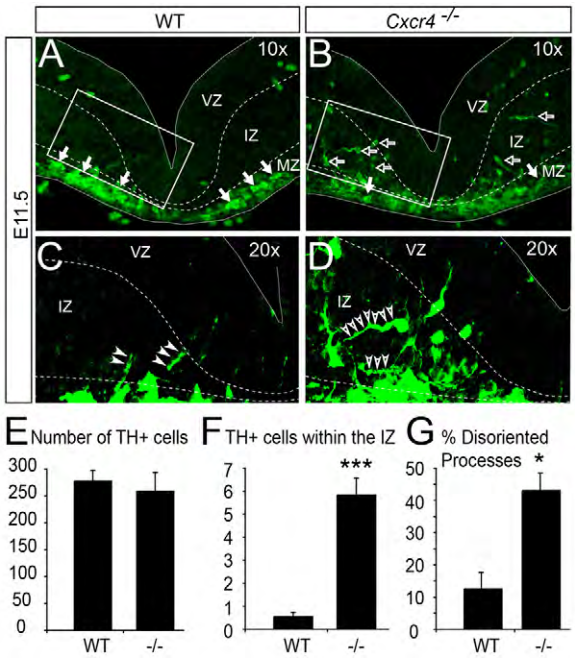

Fig. 7. Altered migration and process orientation of mDA neurons in *Cxcr4* mutant embryos at E11.5. (A-D) Distribution of TH$^+$ (green) mDA neurons in midbrains of wild-type (A,C; *n*=5) and *Cxcr4*$^{-/-}$ (B,D; *n*=5) embryos at E11.5. White arrows in A and B indicate normally positioned TH$^+$ cells in the marginal zone (MZ) aligning along the ventral subpial region. Open arrows in B indicate displaced TH$^+$ cells in intermediate zone (IZ). (C,D) Saturated high magnifications of boxed areas in A and B, respectively. Arrowheads in C show perpendicularly (radially) orientated neurites of TH$^+$ cells in wild-type embryos. Arrowheads in D show disorientated (not perpendicular) neurites of misplaced TH$^+$ cells in *Cxcr4*$^{-/-}$ embryos. (E) Total number of TH$^+$ cells is not altered in *Cxcr4*$^{-/-}$ compared with wild-type embryos. (F) TH$^+$ cell number is higher in the IZ of *Cxcr4*$^{-/-}$ embryos versus wild type. ***P<0.001, *t*-test. (G) More disorientated neurites were detected in *Cxcr4*$^{-/-}$ embryos versus wild type. *P<0.05, *t*-test.

medial forebrain bundle (MFB). In the present study, we first found that VM meninges regulate axonal bundling in organotypic cultures and found CXCR4 phosphorylation in mDA processes at different stages of development, suggestive of an *in vivo* function. In agreement with this, meningeal CXCL12 promoted neuritogenesis in mDA neurons via CXCR4 in explant assays. In our experiments, we found that CXCL12 also promotes neuritogenesis in mDA neurons both *in vitro* and *in vivo*. Indeed, we observed that the TH$^+$ neurites of E11.5 and E14 *Cxcr4*$^{-/-}$ embryos were disoriented and resembled those of cortical neurons when radial migration is interfered with (Chen et al., 2008; Elias et al., 2007). However, CXCL12/CXCR4 has also been described to serve as a permissive mechanism to repulsive signals for axon growth, as described for Slit2, aemaphorin 3A and semaphorin 3C in retinal, dorsal root and sympathetic ganglion neurons, respectively (Chalasani et al., 2003). SEMA3A and SEMA3F are also expressed in the VM (Torre et al., 2010; Prestoz et al., 2012) and induce strong repulsion to mDA axons *in vitro*, but deletion of their receptors, *Nrp1* or *Nrp2*, results in only mild defects in DA axon pathfinding (Torre et al., 2010). These results, together with our data, suggest that mDA axonal growth and neuritogenesis is redundantly regulated by multiple mechanisms, including CXCL12.

Finally, we suggest that CXCL12, by virtue of its role in promoting mDA neuron migration and neuritogenesis, may constitute an interesting tool in regenerative therapy to improve the directed innervation/reinnervation of the striatum in Parkinson's disease. However, this possibility needs to be carefully examined in the light of the known role of CXCL12/CXCR4 in the recruitment of inflammatory cells (Gonzalo et al., 2000; Lukacs et al., 2002). Indeed, it is possible that CXCL12 may contribute to the recruitment of inflammatory cells at the site of a neural transplant, as it has been reported for T lymphocytes in the case of human fetal tissue grafts in individuals with Parkinson's disease (Kordower et al., 2008; Mendez et al., 2008). Future studies should thus aim at ascertaining the role of chemokines in the migration of inflammatory cells and neurons, and the result of this crosstalk between the immune and the neural systems.

In summary, the results presented in this manuscript provide direct evidence to indicate that CXCL12/CXCR4 regulates the radial migration and process outgrowth of mDA neurons during development.

MATERIALS AND METHODS

Animals

Male and female wild-type *CD-1* mice (25-35 g; Charles River) were housed, bred and treated according to directive 86/609/EEC decree 2001-486, Spanish law (32/2007) and local ethical committees: Stockholm Norra Djurförsöksetisks Nämnd (N154/06, N273/11 and N370/09), Instituto de Neurociencias de Alicante and UCSF Committee on Animal Research. *Cxcr4*$^{-/-}$ mice (Zou et al., 1998) were maintained in a *C57b/6* background. Transgenic *Cxcr4-EGFP* mice (Gong et al., 2003) were maintained in a mixed genetic background.

For embryo analyses, wild-type CD-1 mice were mated overnight, and noon of the day the plug was considered E0.5. Embryos were dissected out of the uterine horns in ice-cold PBS, fixed in 4% (wt/wt) paraformaldehyde (PFA) for 4 hours to overnight, cryoprotected in 15-30% sucrose and frozen in Tissue-Tek Optimum Cutting Temperature (OCT) compound (Sakura Fine-Tek) on dry ice. Serial coronal 14 µm sections of the brain were cut using a cryostat.

Immunohistochemical analysis

Sections were pre-incubated for 1 hour in blocking solution followed by incubation at 4°C overnight with following primary antibodies: rabbit anti-GFP (1:1000, Molecular Probes, A-6455), chicken anti-GFP (1:1000, Aves Labs, GFP-1020), guinea pig anti-GLAST (1:200, Millipore, AB1783), rabbit anti-NURR1 (1:200, Santa Cruz, sc-990), mouse anti-NURR1 (1:200, R&D, PP-N1404-00), rabbit anti-TH (1:750, PelFreeze, P40101-0), rabbit anti-SOX2 (1:3000, Thomas Edlund), rabbit anti-LMX1A (1:500, M.S. German), rabbit anti-CXCR4 (1:200, Clone No. UMB-2, Epitomics, 3108-1), mouse anti-nestin (1:200, BD Biosciences, 611659), rabbit anti-S339 CXCR4 (Abcam, ab74012; Sigma-Aldrich, SAB4504153) and rabbit anti-S324/325 CXCR4 (ECM-Biosciences, CP4251). After washing, slides were incubated for 1-2 hours at room temperature with the appropriate fluorophore-conjugated (Cy2-, Cy3-and Cy5-, 1:300, Jackson Laboratories; Alexa488-, 555- and 647-, 1:1000, Invitrogen) secondary antibodies. Confocal pictures were taken with a Zeiss LSM5 EXCITER or LSM700 microscope.

For lambda protein phosphatase (λPP) treatment, sections were incubated with λPP (800U; New England Biolabs) in Protein MetalloPhosphatases buffer with $MnCl_2$ provided by manufacturer for 1 hour at room temperature. Control sections were subjected to the same process except in a buffer without λPP. After λPP treatment, sections were rinsed in PBS three times, followed by regular immunohistochemistry processing.

For the quantification of the distribution of TH$^+$ cells in coronal sections, we divided the VM into eight compartments: ventricular zone (VZ), upper and lower intermediate zones (uIZ and lIZ), marginal zone (MZ) and midline region. Brain sections were counterstained with DAPI to reveal difference in cell distribution and density within the VM. First, low cell density regions were determined (supplementary material Fig. S3A,B). In step 2, Lines aa′, ab, cc′ and cd were drawn following the low density areas.

Development (2013) doi:10.1242/dev.098145

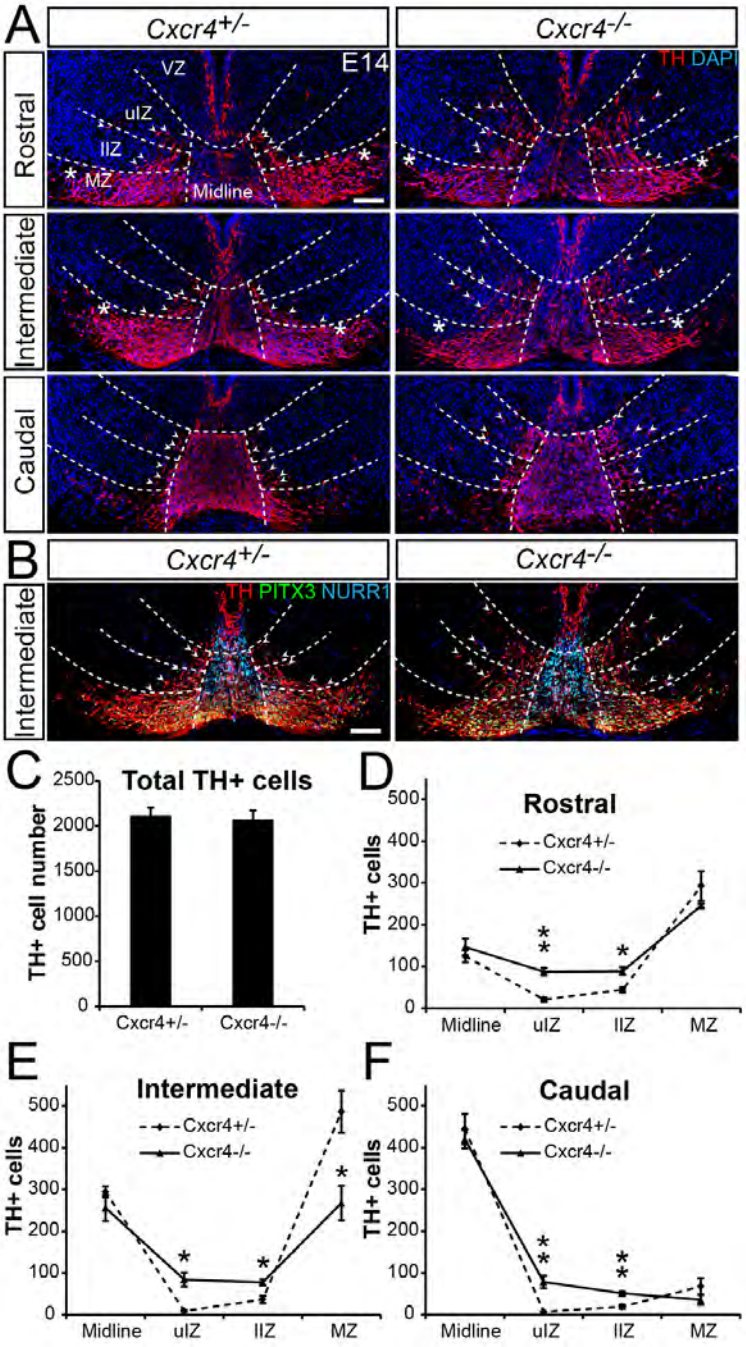

Fig. 8. mDA neurons are retained in the lZ of *Cxcr4* mutant embryos at E14. (A) Distribution of TH$^+$ (red) mDA neurons in midbrains of *Cxcr4*$^{+/-}$ and *Cxcr4*$^{-/-}$ (*n*=3 for each group) embryos at three rostrocaudal levels (rostral, intermediate and caudal) at E14. Asterisks indicate the same distance from the midline. (B) TH$^+$ cells co-express NURR1 and PITX3 in *Cxcr4*$^{+/-}$ as well as *Cxcr4*$^{-/-}$. Arrowheads (A,B) indicate the most lateral TH$^+$ cells in each compartment. (C) Total number of TH$^+$ cells is not altered. (D-F) Quantification of distributions of TH$^+$ cells in midline region, upper intermediate zone (uIZ), lower intermediate zone (lIZ) and marginal zone (MZ) at rostral (D), intermediate (E) and caudal (F) levels. **P*<0.05, ***P*<0.01, *t*-test. Scale bars: 100 μm. VZ, ventricular zone.

Points e and f, the midpoints of lines ab and cd, respectively, were drawn. Subsequently, points g and h, the midpoints of lines ae and cf, respectively, were also drawn (supplementary material Fig. S3C,D). In step 3, four imaginary lines, i.e. lines 6-9 were drawn starting from points e-h, respectively (supplementary material Fig. S3E,F). Lines 6 and 7 were drawn parallel to brain surface. Lines 3 and 4 were connected by line 5. VMs were divided into eight compartments by these lines.

Western blot

VM tissues of four E11.5 embryos were dissected under stereo microscope and pooled in 50 μl RIPA buffer, sonicated for 5 seconds and centrifuged for 30 minutes at 16,000 ***g*** at 4°C. The lysate was mixed with SDS sample buffer and boiled for 5 minutes. Two aliquots of sample were subjected to 10% SDS-PAGE and transferred onto polyvinyl difluoride membrane. After blocking with 5% BSA, each lane on the membrane was cut. One piece was treated with 800 U of λPP and the other one with the phosphatase buffer. The membranes were detected with UMB-2 or anti-S339 CXCR4 antibodies.

In situ hybridization

For *in situ* hybridization, embryos were fixed (4% PFA, 4°C) overnight before being cryopreserved in 30% sucrose, frozen in OCT and sectioned. *In situ* hybridization was performed as described previously (Conlon and Herrmann, 1993). The following mouse antisense RNA probes were used: *Cxcl12, Cxcr4* (clone number 3483088 and 4457694; Invitrogen), *Ngn2*, *Lmx1b* (Kele et al., 2006) and *Nurr1* (Zetterström et al., 1997).

VM explant cultures

Brains from E11.5 CD-1 mice were embedded in 4% low-melting (Mercury) agarose gel. Coronal sections were cut on a vibratome (VT1000S, Leica). For meninges ablation experiment, slices with or without meninges were then transferred to polycarbonate membranes (8.0 μm pore size; 13 mm;

Whatman) in organ tissue culture dishes containing 1 ml of N2 medium. For neurite outgrowth experiment, ventral halves of the midbrain sections were cut and confronted with a piece of meninges and were cultured in Matrigel matrices (BD Biosciences). For cell migration experiments, midbrain floor plate tissue was cut into pieces. Three or four pieces were confronted with a piece of meninges or COS7 cell aggregates expressing tdTomato (pSUPER-*tdTomato*) or *tdTomato* and *Cxcl12* (pCMV-SPORT-*Cxcl12*), and were cultured in Matrigel matrices. Cultures were fixed for 1 hour in 4% PFA after 48-72 hours in culture. Immunohistochemistry was performed as described above.

In utero electroporation

E12.5 pregnant females were deeply anesthetized using Isofluorane (IsoFlo, Abbott Labs) and the uterine horns were accessed through an abdominal incision. pCAGIG-IRES-*Gfp* or pCAGIG-*Cxcl12*-IRES-*Gfp* plasmids were injected into the mesencephalic ventricle. Plasmids were used at 1 μg/μl in PBS containing 10% of Fast Green (Sigma). Square electric pulses of 30 V and 50 ms were passed through the uterus five times, spaced by 950 ms, using a square pulse electroporator (CUY21, Nepa GENE). The uterine horns were replaced in the abdominal cavity, which was then closed with sutures.

In utero intraventricular injections

For *in vivo* blocking of CXCR4 receptors, surgery was performed as for *in utero* electroporation on embryos at E11.5, and 1 μl of AMD3100 solution (5 mM; Sigma) or vehicle (PBS) was injected into the cerebral aqueduct. Embryos were analyzed 48 hours later.

Acknowledgements

We thank members of the Arenas lab, as well as Paola Sacchetti, Ruani Fernando, Emma Andersson and Linda Andersson for critical reading of the manuscript; Satish Kitambi and Shigeaki Kanatani for constructive discussions on some of the techniques; Songbai Zhang for pSUPER-tdTomato plasmid; Lottie Jansson-Sjöstrand, Johnny Söderlund and Trinidad Gil Garcia for technical assistance; Alessandra Nanni for secretarial assistance.

Competing interests

The authors declare no competing financial interests.

Author contributions

S.Y., L.C.E., J.A.S.-A., N.F., S.B. and J.H. performed experiments and contributed to data analysis and interpretation. S.Y., L.C.E. and E.A. wrote the manuscript. P.U., S.J.P., J.C.V., O.M. and E.A. contributed to experimental design and interpretation. S.J.P. and O.M. contributed reagents. All authors read and approved the final manuscript for publication.

Funding

This work was funded by the Swedish Research Council [VR projects: DBRM, 2008:2811, 2011-3116 and 2011-3318]; by the Swedish Foundation for Strategic Research (SRL program); by the Knut and Alice Wallenberg Foundation (CLICK); by the European Commission (NeuroStemcell and DDPD-Genes) and Karolinska Institutet (SFO Thematic Center in Stem cells and Regenerative Medicine) to E.A.; and by the European Commission [mdDANeurodev 222999] to O.M. S.Y. was supported by grants from KID and Chinese Scholarship Council.

Supplementary material

Supplementary material available online at
http://dev.biologists.org/lookup/suppl/doi:10.1242/dev.098145/-/DC1

References

Albéri, L., Sgadò, P. and Simon, H. H. (2004). Engrailed genes are cell-autonomously required to prevent apoptosis in mesencephalic dopaminergic neurons. *Development* **131**, 3229-3236.

Andersson, E., Tryggvason, U., Deng, Q., Friling, S., Alekseenko, Z., Robert, B., Perlmann, T. and Ericson, J. (2006). Identification of intrinsic determinants of midbrain dopamine neurons. *Cell* **124**, 393-405.

Andersson, E. R., Saltó, C., Villaescusa, J. C., Cajanek, L., Yang, S., Bryjova, L., Nagy, I. I., Vainio, S. J., Ramirez, C., Bryja, V. et al. (2013). Wnt5a cooperates with canonical Wnts to generate midbrain dopaminergic neurons in vivo and in stem cells. *Proc. Natl. Acad. Sci. USA* **110**, E602-E610.

Arakawa, Y., Bito, H., Furuyashiki, T., Tsuji, T., Takemoto-Kimura, S., Kimura, K., Nozaki, K., Hashimoto, N. and Narumiya, S. (2003). Control of axon elongation via an SDF-1alpha/Rho/mDia pathway in cultured cerebellar granule neurons. *J. Cell Biol.* **161**, 381-391.

Balabanian, K., Lagane, B., Infantino, S., Chow, K. Y. C., Harriague, J., Moepps, B., Arenzana-Seisdedos, F., Thelen, M. and Bachelerie, F. (2005). The chemokine SDF-1/CXCL12 binds to and signals through the orphan receptor RDC1 in T lymphocytes. *J. Biol. Chem.* **280**, 35760-35766.

Blakely, B. D., Bye, C. R., Fernando, C. V., Horne, M. K., Macheda, M. L., Stacker, S. A., Arenas, E. and Parish, C. L. (2011). Wnt5a regulates midbrain dopaminergic axon growth and guidance. *PLoS ONE* **6**, e18373.

Bonilla, S., Hall, A. C., Pinto, L., Attardo, A., Götz, M., Huttner, W. B. and Arenas, E. (2008). Identification of midbrain floor plate radial glia-like cells as dopaminergic progenitors. *Glia* **56**, 809-820.

Borrell, V. and Marín, O. (2006). Meninges control tangential migration of hem-derived Cajal-Retzius cells via CXCL12/CXCR4 signaling. *Nat. Neurosci.* **9**, 1284-1293.

Busillo, J. M., Armando, S., Sengupta, R., Meucci, O., Bouvier, M. and Benovic, J. L. (2010). Site-specific phosphorylation of CXCR4 is dynamically regulated by multiple kinases and results in differential modulation of CXCR4 signaling. *J. Biol. Chem.* **285**, 7805-7817.

Castillo, S. O., Baffi, J. S., Palkovits, M., Goldstein, D. S., Kopin, I. J., Witta, J., Magnuson, M. A. and Nikodem, V. M. (1998). Dopamine biosynthesis is selectively abolished in substantia nigra/ventral tegmental area but not in hypothalamic neurons in mice with targeted disruption of the Nurr1 gene. *Mol. Cell. Neurosci.* **11**, 36-46.

Chalasani, S. H., Sabelko, K. A., Sunshine, M. J., Littman, D. R. and Raper, J. A. (2003). A chemokine, SDF-1, reduces the effectiveness of multiple axonal repellents and is required for normal axon pathfinding. *J. Neurosci.* **23**, 1360-1371.

Chen, G., Sima, J., Jin, M., Wang, K.-Y., Xue, X.-J., Zheng, W., Ding, Y.-Q. and Yuan, X.-B. (2008). Semaphorin-3A guides radial migration of cortical neurons during development. *Nat. Neurosci.* **11**, 36-44.

Conlon, R. A. and Herrmann, B. G. (1993). Detection of messenger RNA by in situ hybridization to postimplantation embryo whole mounts. *Methods Enzymol.* **225**, 373-383.

Deng, Q., Andersson, E., Hedlund, E., Alekseenko, Z., Coppola, E., Panman, L., Millonig, J. H., Brunet, J.-F., Ericson, J. and Perlmann, T. (2011). Specific and integrated roles of Lmx1a, Lmx1b and Phox2a in ventral midbrain development. *Development* **138**, 3399-3408.

Di Salvio, M., Di Giovannantonio, L. G., Acampora, D., Prosperi, R., Omodei, D., Prakash, N., Wurst, W. and Simeone, A. (2010). Otx2 controls neuron subtype identity in ventral tegmental area and antagonizes vulnerability to MPTP. *Nat. Neurosci.* **13**, 1481-1488.

Elias, L. A., Wang, D. D. and Kriegstein, A. R. (2007). Gap junction adhesion is necessary for radial migration in the neocortex. *Nature* **448**, 901-907.

Fischer, T., Nagel, F., Jacobs, S., Stumm, R. and Schulz, S. (2008). Reassessment of CXCR4 chemokine receptor expression in human normal and neoplastic tissues using the novel rabbit monoclonal antibody UMB-2. *PLoS ONE* **3**, e4069.

Gerlach, L. O., Skerlj, R. T., Bridger, G. J. and Schwartz, T. W. (2001). Molecular interactions of cyclam and bicyclam non-peptide antagonists with the CXCR4 chemokine receptor. *J. Biol. Chem.* **276**, 14153-14160.

Gong, S., Zheng, C., Doughty, M. L., Losos, K., Didkovsky, N., Schambra, U. B., Nowak, N. J., Joyner, A., Leblanc, G., Hatten, M. E. et al. (2003). A gene expression atlas of the central nervous system based on bacterial artificial chromosomes. *Nature* **425**, 917-925.

Gonzalo, J. A., Lloyd, C. M., Peled, A., Delaney, T., Coyle, A. J. and Gutierrez-Ramos, J. C. (2000). Critical involvement of the chemotactic axis CXCR4/stromal cell-derived factor-1 alpha in the inflammatory component of allergic airway disease. *J. Immunol.* **165**, 499-508.

Guyon, A., Skrzydelski, D., Rovère, C., Apartis, E., Rostène, W., Kitabgi, P., Mélik Parsadaniantz, S. and Nahon, J. L. (2008). Stromal-cell-derived factor 1alpha /CXCL12 modulates high-threshold calcium currents in rat substantia nigra. *Eur. J. Neurosci.* **28**, 862-870.

Hanaway, J., McConnell, J. A. and Netsky, M. G. (1971). Histogenesis of the substantia nigra, ventral tegmental area of Tsai and interpeduncular nucleus: an autoradiographic study of the mesencephalon in the rat. *J. Comp. Neurol.* **142**, 59-73.

Hatse, S., Princen, K., Bridger, G., De Clercq, E. and Schols, D. (2002). Chemokine receptor inhibition by AMD3100 is strictly confined to CXCR4. *FEBS Lett.* **527**, 255-262.

Ikemoto, S. and Panksepp, J. (1999). The role of nucleus accumbens dopamine in motivated behavior: a unifying interpretation with special reference to reward-seeking. *Brain Res. Brain Res. Rev.* **31**, 6-41.

Inestrosa, N. C. and Arenas, E. (2010). Emerging roles of Wnts in the adult nervous system. *Nat. Rev. Neurosci.* **11**, 77-86.

Kawano, H., Ohyama, K., Kawamura, K. and Nagatsu, I. (1995). Migration of dopaminergic neurons in the embryonic mesencephalon of mice. *Brain Res. Dev. Brain Res.* **86**, 101-113.

Kele, J., Simplicio, N., Ferri, A. L. M., Mira, H., Guillemot, F., Arenas, E. and Ang, S.-L. (2006). Neurogenin 2 is required for the development of ventral midbrain dopaminergic neurons. *Development* **133**, 495-505.

Knaut, H., Blader, P., Strähle, U. and Schier, A. F. (2005). Assembly of trigeminal sensory ganglia by chemokine signaling. *Neuron* **47**, 653-666.

Kolk, S. M., Gunput, R.-A. F., Tran, T. S., van den Heuvel, D. M., Prasad, A. A., Hellemons, A. J., Adolfs, Y., Ginty, D. D., Kolodkin, A. L., Burbach, J. P. et al. (2009). Semaphorin 3F is a bifunctional guidance cue for dopaminergic axons and controls their fasciculation, channeling, rostral growth, and intracortical targeting. *J. Neurosci.* **29**, 12542-12557.

Kordower, J. H., Chu, Y., Hauser, R. A., Freeman, T. B. and Olanow, C. W. (2008). Lewy body-like pathology in long-term embryonic nigral transplants in Parkinson's disease. *Nat. Med.* **14**, 504-506.

Lazarini, F., Casanova, P., Tham, T. N., De Clercq, E., Arenzana-Seisdedos, F., Baleux, F. and Dubois-Dalcq, M. (2000). Differential signalling of the chemokine receptor CXCR4 by stromal cell-derived factor 1 and the HIV glycoprotein in rat neurons and astrocytes. *Eur. J. Neurosci.* **12**, 117-125.

Lerner, O., Davenport, D., Patel, P., Psatha, M., Lieberam, I. and Guthrie, S. (2010). Stromal cell-derived factor-1 and hepatocyte growth factor guide axon projections to the extraocular muscles. *Dev. Neurobiol.* **70**, 549-564.

Li, Q., Shirabe, K., Thisse, C., Thisse, B., Okamoto, H., Masai, I. and Kuwada, J. Y. (2005). Chemokine signaling guides axons within the retina in zebrafish. *J. Neurosci.* **25**, 1711-1717.

Li, G., Kataoka, H., Coughlin, S. R. and Pleasure, S. J. (2009). Identification of a transient subpial neurogenic zone in the developing dentate gyrus and its regulation by Cxcl12 and reelin signaling. *Development* **136**, 327-335.

Liapi, A., Pritchett, J., Jones, O., Fujii, N., Parnavelas, J. G. and Nadarajah, B. (2008). Stromal-derived factor 1 signalling regulates radial and tangential migration in the developing cerebral cortex. *Dev. Neurosci.* **30**, 117-131.

Lieberam, I., Agalliu, D., Nagasawa, T., Ericson, J. and Jessell, T. M. (2005). A Cxcl12-CXCR4 chemokine signaling pathway defines the initial trajectory of mammalian motor axons. *Neuron* **47**, 667-679.

López-Bendito, G., Sánchez-Alcañiz, J. A., Pla, R., Borrell, V., Picó, E., Valdeolmillos, M. and Marín, O. (2008). Chemokine signaling controls intracortical migration and final distribution of GABAergic interneurons. *J. Neurosci.* **28**, 1613-1624.

Lu, M., Grove, E. A. and Miller, R. J. (2002). Abnormal development of the hippocampal dentate gyrus in mice lacking the CXCR4 chemokine receptor. *Proc. Natl. Acad. Sci. USA* **99**, 7090-7095.

Lukacs, N. W., Berlin, A., Schols, D., Skerlj, R. T. and Bridger, G. J. (2002). AMD3100, a CxCR4 antagonist, attenuates allergic lung inflammation and airway hyperreactivity. *Am. J. Pathol.* **160**, 1353-1360.

Ma, Q., Jones, D., Borghesani, P. R., Segal, R. A., Nagasawa, T., Kishimoto, T., Bronson, R. T. and Springer, T. A. (1998). Impaired B-lymphopoiesis, myelopoiesis, and derailed cerebellar neuron migration in CXCR4- and SDF-1-deficient mice. *Proc. Natl. Acad. Sci. USA* **95**, 9448-9453.

Mélik-Parsadaniantz, S. and Rostène, W. (2008). Chemokines and neuromodulation. *J. Neuroimmunol.* **198**, 62-68.

Mendez, I., Viñuela, A., Astradsson, A., Mukhida, K., Hallett, P., Robertson, H., Tierney, T., Holness, R., Dagher, A., Trojanowski, J. Q. et al. (2008). Dopamine neurons implanted into people with Parkinson's disease survive without pathology for 14 years. *Nat. Med.* **14**, 507-509.

Mithal, D. S., Banisadr, G. and Miller, R. J. (2012). CXCL12 signaling in the development of the nervous system. *J. Neuroimmune Pharmacol.* **7**, 820-834.

Miyasaka, N., Knaut, H. and Yoshihara, Y. (2007). Cxcl12/Cxcr4 chemokine signaling is required for placode assembly and sensory axon pathfinding in the zebrafish olfactory system. *Development* **134**, 2459-2468.

Mueller, W., Schütz, D., Nagel, F., Schulz, S. and Stumm, R. (2013). Hierarchical organization of multi-site phosphorylation at the CXCR4 C terminus. *PLoS ONE* **8**, e64975.

Odemis, V., Lamp, E., Pezeshki, G., Moepps, B., Schilling, K., Gierschik, P., Littman, D. R. and Engele, J. (2005). Mice deficient in the chemokine receptor CXCR4 exhibit impaired limb innervation and myogenesis. *Mol. Cell. Neurosci.* **30**, 494-505.

Paredes, M. F., Li, G., Berger, O., Baraban, S. C. and Pleasure, S. J. (2006). Stromal-derived factor-1 (CXCL12) regulates laminar position of Cajal-Retzius cells in normal and dysplastic brains. *J. Neurosci.* **26**, 9404-9412.

Prakash, N. and Wurst, W. (2006). Genetic networks controlling the development of midbrain dopaminergic neurons. *J. Physiol.* **575**, 403-410.

Prestoz, L., Jaber, M. and Gaillard, A. (2012). Dopaminergic axon guidance: which makes what? *Front. Cell. Neurosci.* **6**, 32.

Reiss, K., Mentlein, R., Sievers, J. and Hartmann, D. (2002). Stromal cell-derived factor 1 is secreted by meningeal cells and acts as chemotactic factor on neuronal stem cells of the cerebellar external granular layer. *Neuroscience* **115**, 295-305.

Rubin, J. B., Kung, A. L., Klein, R. S., Chan, J. A., Sun, Y., Schmidt, K., Kieran, M. W., Luster, A. D. and Segal, R. A. (2003). A small-molecule antagonist of CXCR4 inhibits intracranial growth of primary brain tumors. *Proc. Natl. Acad. Sci. USA* **100**, 13513-13518.

Sánchez-Alcañiz, J. A., Haege, S., Mueller, W., Pla, R., Mackay, F., Schulz, S., López-Bendito, G., Stumm, R. and Marín, O. (2011). Cxcr7 controls neuronal migration by regulating chemokine responsiveness. *Neuron* **69**, 77-90.

Sapède, D., Rossel, M., Dambly-Chaudière, C. and Ghysen, A. (2005). Role of SDF1 chemokine in the development of lateral line efferent and facial motor neurons. *Proc. Natl. Acad. Sci. USA* **102**, 1714-1718.

Saucedo-Cardenas, O., Quintana-Hau, J. D., Le, W. D., Smidt, M. P., Cox, J. J., De Mayo, F., Burbach, J. P. and Conneely, O. M. (1998). Nurr1 is essential for the induction of the dopaminergic phenotype and the survival of ventral mesencephalic late dopaminergic precursor neurons. *Proc. Natl. Acad. Sci. USA* **95**, 4013-4018.

Schols, D., Struyf, S., Van Damme, J., Esté, J. A., Henson, G. and De Clercq, E. (1997). Inhibition of T-tropic HIV strains by selective antagonization of the chemokine receptor CXCR4. *J. Exp. Med.* **186**, 1383-1388.

Skrzydelski, D., Guyon, A., Daugé, V., Rovère, C., Apartis, E., Kitabgi, P., Nahon, J. L., Rostène, W. and Parsadaniantz, S. M. (2007). The chemokine stromal cell-derived factor-1/CXCL12 activates the nigrostriatal dopamine system. *J. Neurochem.* **102**, 1175-1183.

Smidt, M. P., Asbreuk, C. H., Cox, J. J., Chen, H., Johnson, R. L. and Burbach, J. P. (2000). A second independent pathway for development of mesencephalic dopaminergic neurons requires Lmx1b. *Nat. Neurosci.* **3**, 337-341.

Smits, S. M., Burbach, J. P. H. and Smidt, M. P. (2006). Developmental origin and fate of meso-diencephalic dopamine neurons. *Prog. Neurobiol.* **78**, 1-16.

Stumm, R. and Höllt, V. (2007). CXC chemokine receptor 4 regulates neuronal migration and axonal pathfinding in the developing nervous system: implications for neuronal regeneration in the adult brain. *J. Mol. Endocrinol.* **38**, 377-382.

Stumm, R., Kolodziej, A., Schulz, S., Kohtz, J. D. and Höllt, V. (2007). Patterns of SDF-1alpha and SDF-1gamma mRNAs, migration pathways, and phenotypes of CXCR4-expressing neurons in the developing rat telencephalon. *J. Comp. Neurol.* **502**, 382-399.

Sun, Y., Cheng, Z., Ma, L. and Pei, G. (2002). Beta-arrestin2 is critically involved in CXCR4-mediated chemotaxis, and this is mediated by its enhancement of p38 MAPK activation. *J. Biol. Chem.* **277**, 49212-49219.

Tham, T. N., Lazarini, F., Franceschini, I. A., Lachapelle, F., Amara, A. and Dubois-Dalcq, M. (2001). Developmental pattern of expression of the alpha chemokine stromal cell-derived factor 1 in the rat central nervous system. *Eur. J. Neurosci.* **13**, 845-856.

Theofilopoulos, S., Wang, Y., Kitambi, S. S., Sacchetti, P., Sousa, K. M., Bodin, K., Kirk, J., Saltó, C., Gustafsson, M., Toledo, E. M. et al. (2013). Brain endogenous liver X receptor ligands selectively promote midbrain neurogenesis. *Nat. Chem. Biol.* **9**, 126-133.

Tissir, F., Wang, C.-E. and Goffinet, A. M. (2004). Expression of the chemokine receptor Cxcr4 mRNA during mouse brain development. *Brain Res. Dev. Brain Res.* **149**, 63-71.

Tiveron, M.-C., Rossel, M., Moepps, B., Zhang, Y. L., Seidenfaden, R., Favor, J., König, N. and Cremer, H. (2006). Molecular interaction between projection neuron precursors and invading interneurons via stromal-derived factor 1 (CXCL12)/CXCR4 signaling in the cortical subventricular zone/intermediate zone. *J. Neurosci.* **26**, 13273-13278.

Torre, E. R., Gutekunst, C.-A. and Gross, R. E. (2010). Expression by midbrain dopamine neurons of Sema3A and 3F receptors is associated with chemorepulsion in vitro but a mild in vivo phenotype. *Mol. Cell. Neurosci.* **44**, 135-153.

Tysseling, V. M., Mithal, D., Sahni, V., Birch, D., Jung, H., Belmadani, A., Miller, R. J. and Kessler, J. A. (2011). SDF1 in the dorsal corticospinal tract promotes CXCR4+ cell migration after spinal cord injury. *J. Neuroinflammation* **8**, 16.

Van den Heuvel, D. M. and Pasterkamp, R. J. (2008). Getting connected in the dopamine system. *Prog. Neurobiol.* **85**, 75-93.

Xiang, Y., Li, Y., Zhang, Z., Cui, K., Wang, S., Yuan, X. B., Wu, C. P., Poo, M. M. and Duan, S. (2002). Nerve growth cone guidance mediated by G protein-coupled receptors. *Nat. Neurosci.* **5**, 843-848.

Zetterström, R. H., Solomin, L., Jansson, L., Hoffer, B. J., Olson, L. and Perlmann, T. (1997). Dopamine neuron agenesis in Nurr1-deficient mice. *Science* **276**, 248-250.

Zhu, Y. and Murakami, F. (2012). Chemokine CXCL12 and its receptors in the developing central nervous system: emerging themes and future perspectives. *Dev. Neurobiol.* **72**, 1349-1362.

Zhu, Y., Yu, T., Zhang, X.-C., Nagasawa, T., Wu, J. Y. and Rao, Y. (2002). Role of the chemokine SDF-1 as the meningeal attractant for embryonic cerebellar neurons. *Nat. Neurosci.* **5**, 719-720.

Zlotnik, A. and Yoshie, O. (2000). Chemokines: a new classification system and their role in immunity. *Immunity* **12**, 121-127.

Zou, Y. R., Kottmann, A. H., Kuroda, M., Taniuchi, I. and Littman, D. R. (1998). Function of the chemokine receptor CXCR4 in haematopoiesis and in cerebellar development. *Nature* **393**, 595-599.

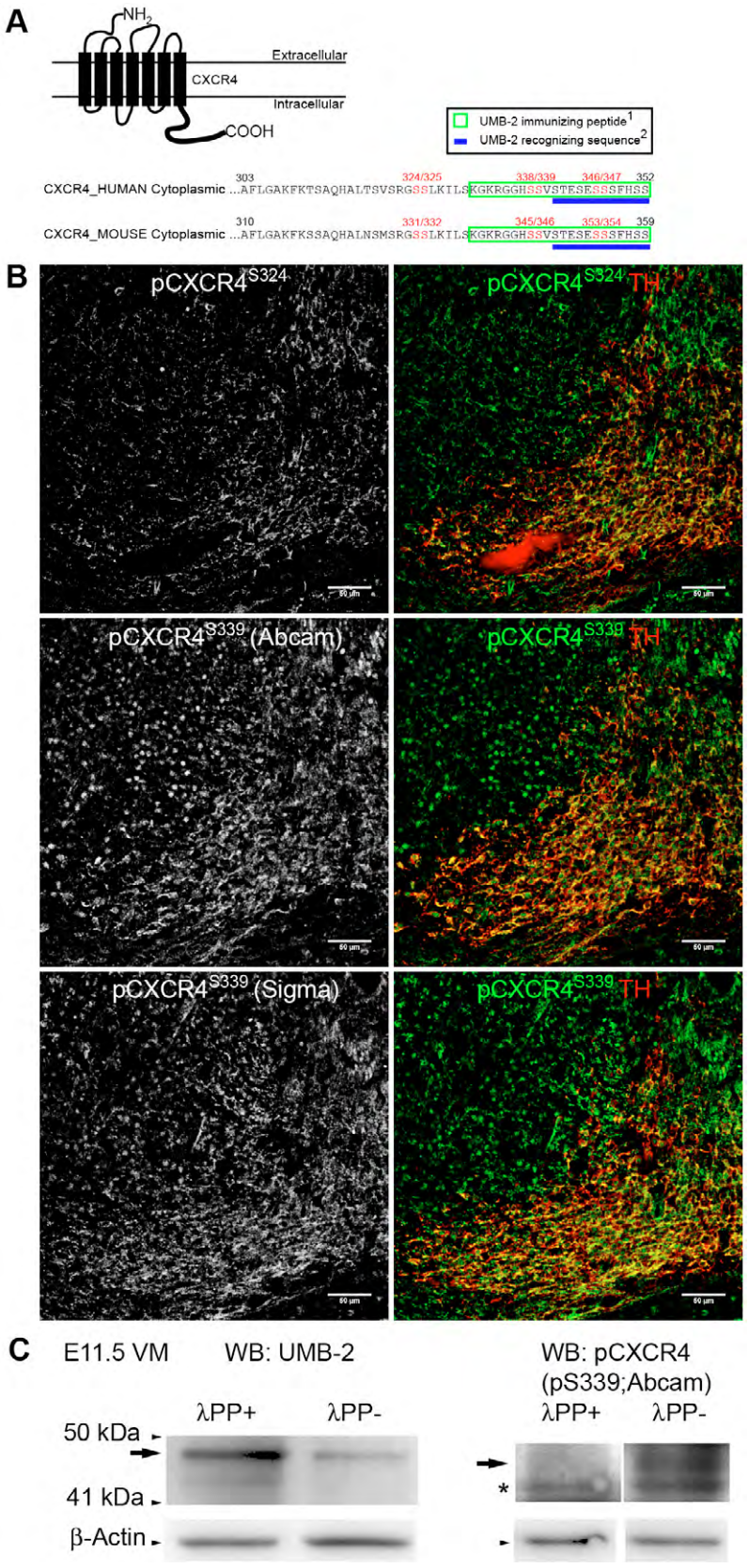

Figure S1. CXCR4 is phosphorylated in developing VM.
(A) Schematic representation of the phosphorylation sites (serine residues in red) of cytoplasmic C-termini of human and mouse CXCR4 and immunizing peptide and epitope of UMB-2 antibody. (B) Immunostaining with antibodies recognizing phosphorylated CXCR4 in S324 or S339 in coronal sections of E13 mouse midbrain. Two CXCR4^{pS339} antibodies manufactured from Abcam and Sigma-Aldrich were used to detect phosphorylated and active CXCR4. (C) Western blot of ventral midbrain of E11.5 mouse was lysates showing phosphatase (λPP) treatment increases the detection of CXCR4 with the UMB-2 antibody and decreases the detection with anti-S339 (Abcam). Arrows indicate the CXCR4 bands. Asterisk (*): non-specific band. Scale bars in B: 50 μm.

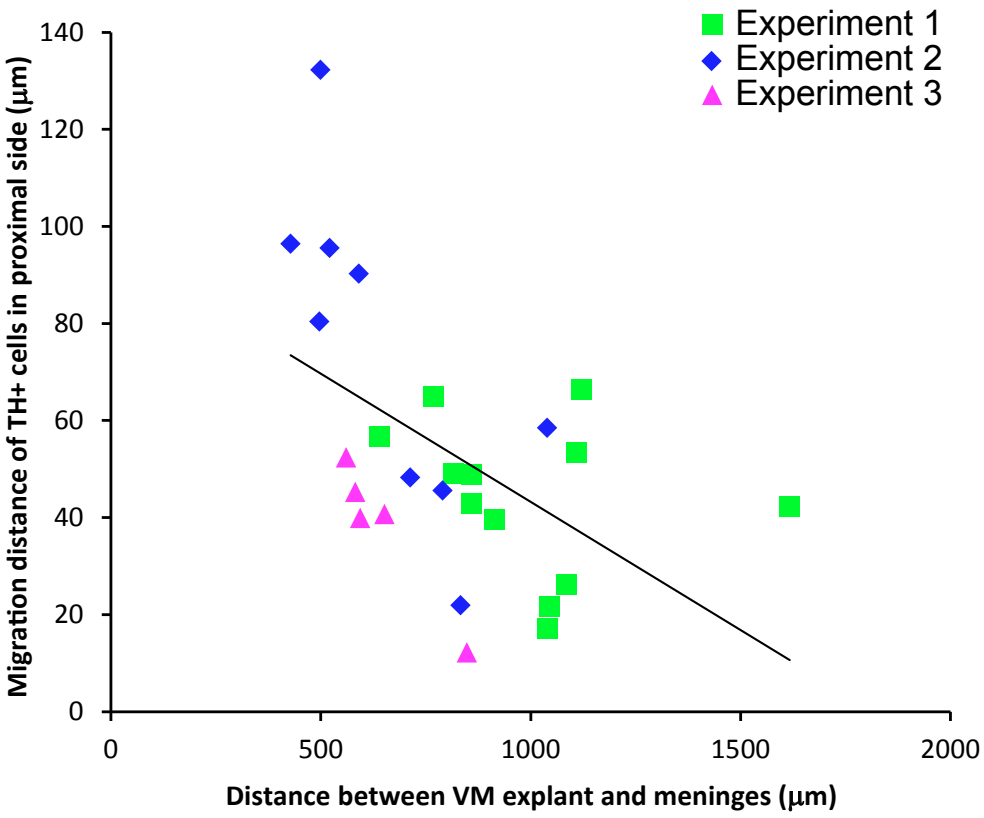

Figure S2. Correlation between the explant-meninge distance and the migration of TH$^+$ cells towards the meninges.
The meninges-explant distance and the proximal migration of TH$^+$ cells towards the meninges at E11.5 are plotted (3 experiments; 26 explants). We found that TH$^+$ cells migrated longer distances the closer they are to the meninges. Pearson correlation test, r = -0.513 and $P < 0.01$.

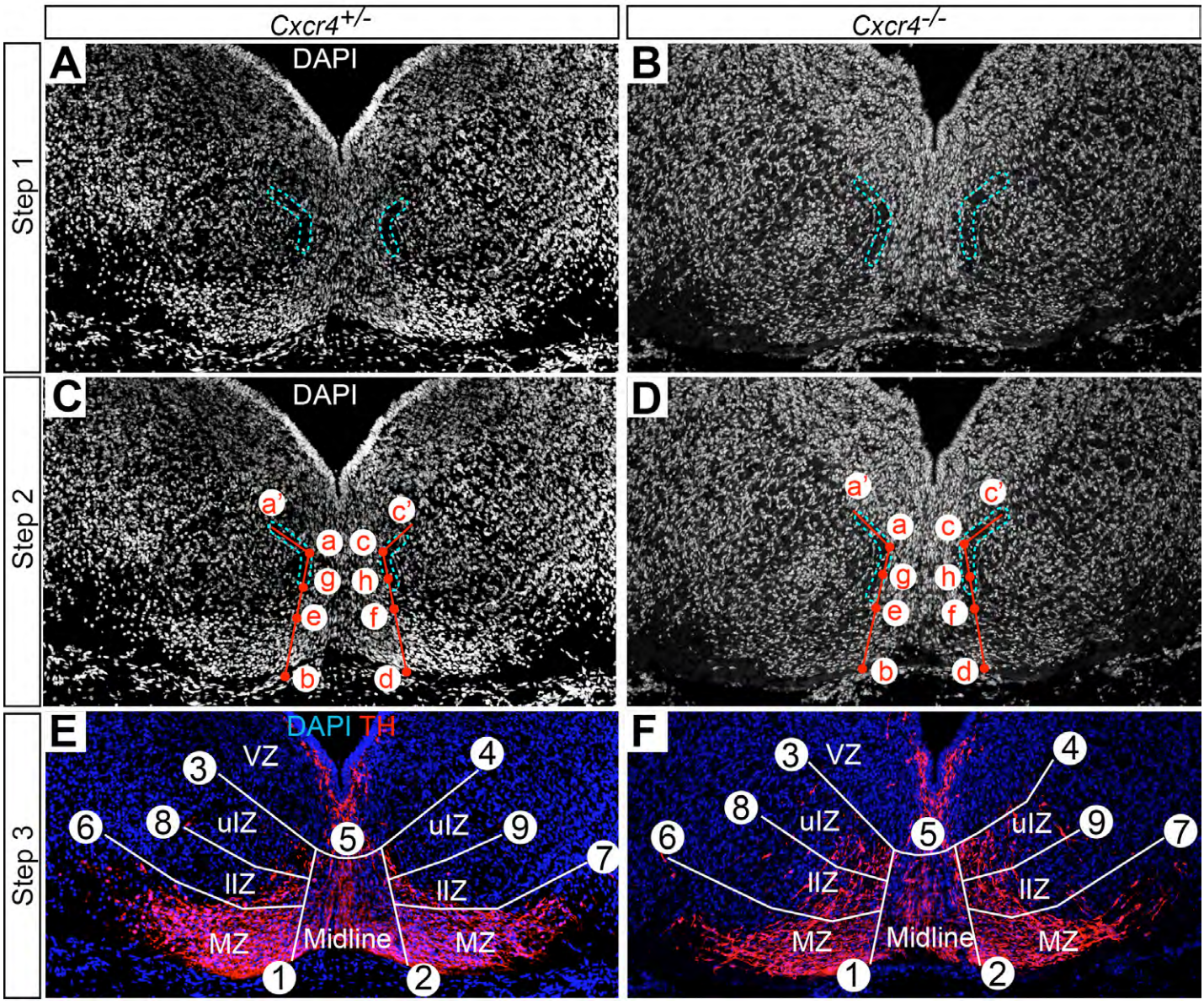

Figure S3. Distribution of TH$^+$ cells in 8 VM compartments in coronal sections.
Compartments were defined in DAPI-counterstained coronal sections. Pictures show intermediate levels of *Cxcr4*$^{+/-}$ (A,C,E) and *Cxcr4*$^{-/-}$ (B,D,F) E14 embryos. (A,B) Step 1: Low cell density areas are identified. (C,D) Step 2: Lines are drawn following the low density areas, between the VZ and the IZ (aa' and cc') and between the midline and lateral IZ and MZ (ab and cd). The midpoints of lines ab (e) and cd (f), respectively, are drawn. Subsequently, points g and h, the midpoints of lines ae and cf, respectively, are also drawn. (E,F) Step 3: Four imaginary lines, ie. line 6,7,8 and 9 are drawn starting from points e,f,g and h, respectively, and parallel to brain surface. Lines 3 and 4 are drawn following the VZ and are connected by line 5.

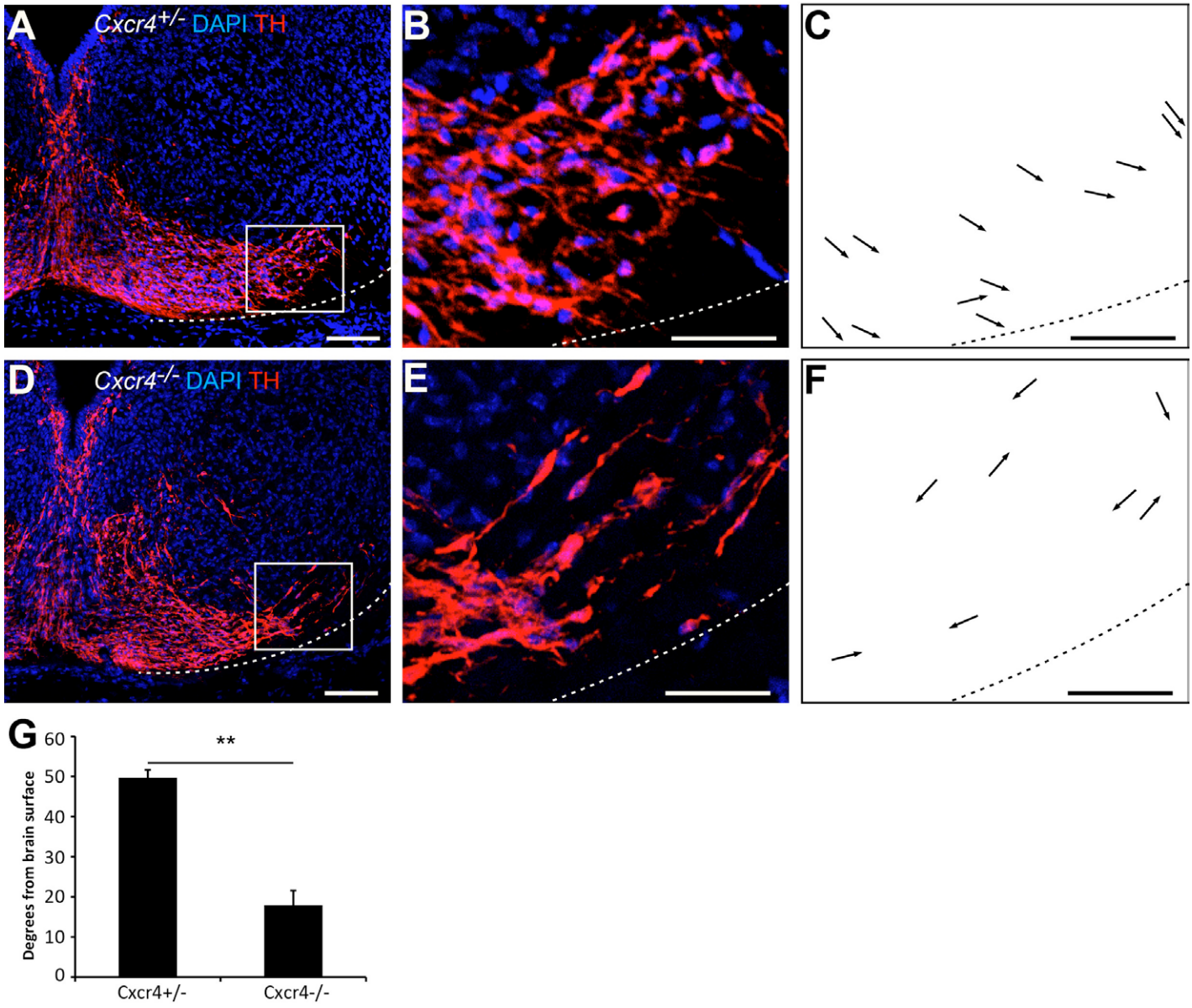

Figure S4. Altered orientation of the TH+ processes in Cxcr4-/- mice at E14.
(A,D) Coronal sections of Cxcr4+/- and Cxcr4-/- VM at E14 were stained with TH (red) and DAPI (blue). B and E are magnified areas of the boxes in A,D, respectively. (C,F) Arrows represent the direction of TH+ processes, starting from the cell bodies, as shown in B and E respectively. Dashed lines in A-F delineate the brain surface. (G) Quantification of the angle, measured in degrees, between TH+ processes and the brain surface showed a very severe alteration in the orientation of TH+ cell processes in Cxcr4-/- embryos. **, $P < 0.01$, t-test. Scale bars: 100 μm (A,D); 50 μm (B,C,E,F).

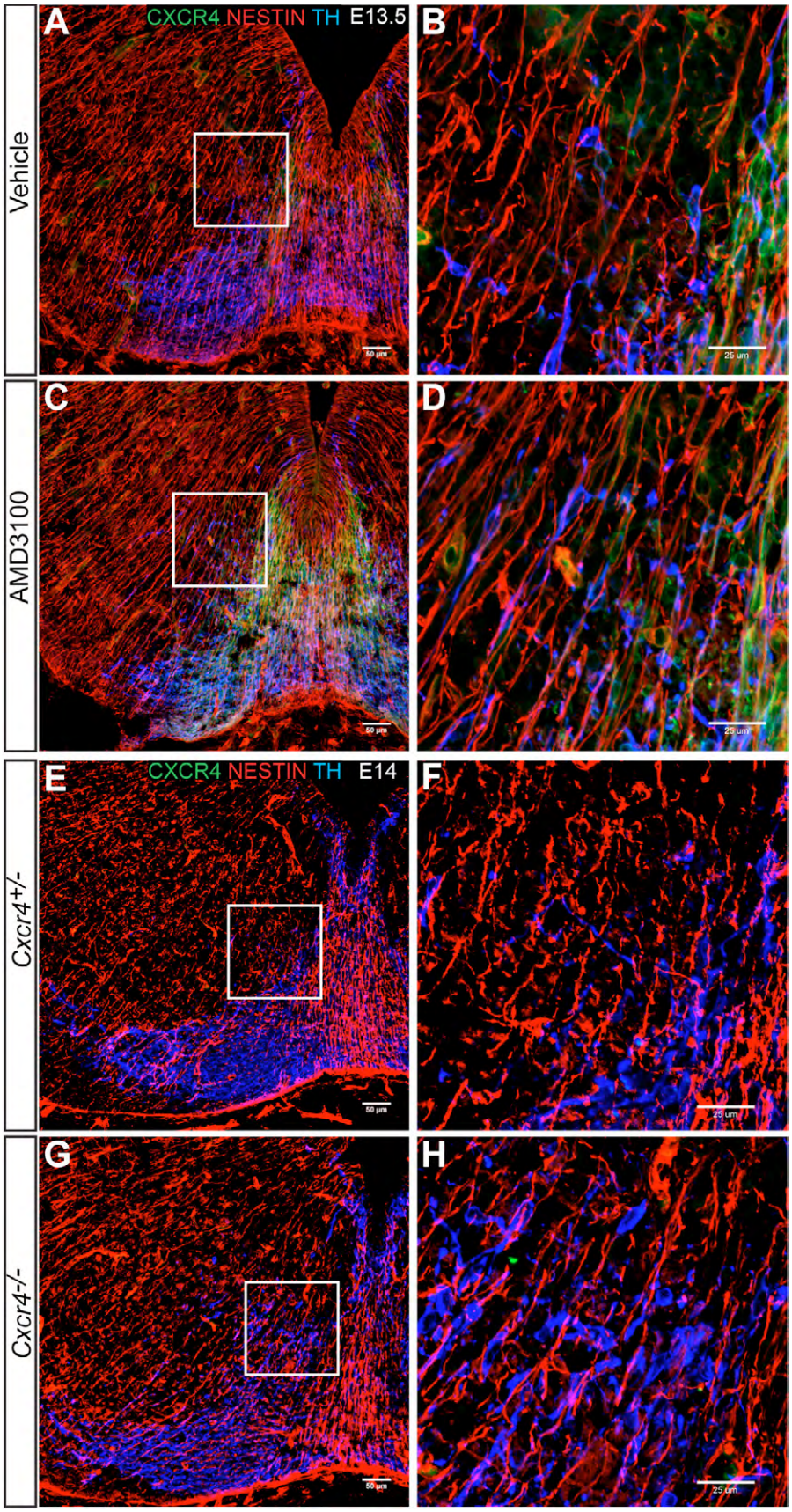

Figure S5. Radial glia is not affected in the VM of either AMD3100-treated or Cxcr4-/- embryos.
(A,C) NESTIN (red) immunostaining in the coronal midbrain sections of Vehicle (A) or AMD3100-injected (B) E13.5 embryos. Boxed areas in A,C are magnified in B,D, respectively. (E,G) NESTIN (red) immunostaining in the coronal midbrain sections of Cxcr4+/- (A) or Cxcr4-/- (B) embryos at E14. Boxed areas in E,G are magnified in F,H, respectively. CXCR4 is in green and TH in blue. Scale bars: 50 μm (A,C,E,G); 25 μm (B,D,F,H).